INVESTIGATION OF THE DETONATION OF ALUMINUM POWDER-OXYGEN MIXTURES

DISSERTATION

Presented in Partial Fulfillment of the Requirements for the Degree of Doctor of Philosophy in the Graduate School of The Ohio State University

by

William Anthony Strauss, B. of M.E., M.Sc.

* * * * *

The Ohio State University

1966

Approved by

R. Edse.

Adviser
Department of Aeronautical and Astronautical Engineering

ACKNOWLEDGMENTS

The author acknowledges and is grateful for the encouragement and advice of his adviser, Dr. R. Edse, during the course of this study. It is also acknowledged that Mr. J. W. Pliickebaum aided in the construction of the experimental apparatus and that Messrs. Orkins and Lawrence aided in the collecting of the experimental data.

This study was supported in part by the National Science Foundation on Research Grants GK 143 and GP 635 with The Ohio State University Research Foundation. Computer time for the theoretical calculations was donated by The Ohio State University Computer Center, Dr. Roy Reeves, Director.

CONTENTS

ILLUSTRATIONS

TABLES

SECTION I

INTRODUCTION

The phenomenon of detonation waves propagating in explosive solids and explosive gas mixtures has been observed and studied for many years. A detonation wave is characterized by a high speed shock wave which propagates through a combustible mixture and is followed by a flame. The shock wave is sustained by the energy released in the exothermic reactions in the flame zone. The mechanism of initiation of detonation in homogeneous gas mixtures is similar to that of generating a shock wave. The accepted model of shock wave generation was first proposed by Becker[1] who suggested that shock waves result from a coalescence of infinitesimal pressure waves. The result of many pressure waves overtaking one another is a wave of supersonic velocity and finite pressure difference between initial and final states. The energy required to produce shock waves may be supplied by an external source such as an accelerating piston. By contrast, the driving force which produces a detonation wave is the accelerating flame front. Since a detonation wave is supersonic, rapid chemical reactions are required to sustain the chemical process. The normal flame speed of a system is an indicator of the overall rate of chemical reactions of that

system; that is, systems having high normal burning rates have fast reaction rates and vise versa.

Only recently have heterogeneous liquid fuel-gas oxidizer mixtures been studied with respect to detonation. In all of these cases, the studies were conducted by passing high energy shock waves through the mixtures. Kling and Maman[2] studied the kerosene-air system. For a stoichiometric mixture, they observed detonation, but only after reflection of the incident shock. The observed velocities agreed with theoretical values. Cramer[3] reported observing "detonation like" waves propagating through DECH (diethylcyclohexane, $C_{10}H_{20}$) fuel spray-oxygen mixtures. Frazer[4] was able to detonate both octane-oxygen and benzene-oxygen mixtures (also initiated with a high energy shock wave). Nichols, Dabora and Ragland[5] also reported "detonation like" waves in heterogeneous DECH-oxygen mixtures. While it is difficult to produce detonations in the above heterogeneous liquid-gas mixtures, it would appear that to detonate powdered metal fuel-gas oxidizer mixtures would be even more difficult.

The combustion of metal powders in gaseous atmospheres was first studied by Hartman and Greenwald of the Bureau of Mines in 1945.[6] They reported that finely divided aluminum powder is easy to ignite and will react in gas atmospheres of air, oxygen, carbon dioxide and in special cases, nitrogen. They also reported that the burning of aluminum

occurred with a violent explosion. Cassell, Das Gupta and Guruswamy[7] measured the burning velocities of powdered aluminum in various oxygen-nitrogen atmospheres. For a 70 percent oxygen, 30 percent nitrogen atmosphere, they reported "tube" burning velocities of approximately 40 cm/sec. Bunsen-burner flame velocities of aluminum powder-oxygen mixtures were measured earlier at this laboratory (Appendix III) and found to be approximately 25 cm/sec. The low burning velocities of this system result from the slow overall reaction rates. The initial surface reaction is believed to be the rate limiting mechanism. These low burning rates suggest that it would be very difficult for such a system to self-initiate a detonation as well as to support a detonation if initiated by other methods. Grosse and Conway[8] conducted a study of some of the properties of combustion of aluminum-oxygen mixtures while developing a high temperature cutting torch. These torches were subsequently used to cut through concrete blocks several feet thick. The continuum radiation emitted by the Bunsen-burner flames of this system was studied at this laboratory and was found equal to that of a carbon arc operating at 50 volts and 10 amperes.[9]

In recent years, the interest in aluminum powder combustion has increased because of its usefulness as a fuel additive and combustion stablizer in solid rocket propellants. The properties of the oxides of aluminum have also been under

investigation[10,11] and tables of their thermodynamic values have been compiled.

It was generally assumed that the very low burning velocities (slow reaction rates) of the powder-gas mixtures preclude the formation of detonation waves in such mixtures. However, in the course of the aluminum powder-oxygen Bunsen-burner flame work at this laboratory (Appendix III, Reference 9), there was some evidence that these mixtures detonated when their flames entered the burner tubes. The purpose of the present investigation was to establish whether these mixtures are detonable and if so, to study their properties experimentally and theoretically.

SECTION II

APPARATUS, INSTRUMENTATION AND METHOD

In an effort to establish detonation waves in the heterogeneous aluminum powder-oxygen mixtures, flames were allowed to propagate through these mixtures in long tubes. This technique has been used successfully for the study of the detonation properties of homogeneous gas mixtures. The equipment used for these experiments includes a long glass tube, a system to fill this tube with the aluminum-oxygen mixture, an ignitor at one end of the tube and the necessary instrumentation. After a uniform aluminum-oxygen mixture has been established in the tube, the ignitor is set off. With a low energy ignitor, a combustion wave is formed initially. This combustion wave then speeds up and leads to a detonation wave after it has traversed a certain distance which is called the detonation induction distance.

Apparatus

A sketch of the apparatus is shown in Figure 1. For regulating and metering the oxygen gas flow, a pressure reducing regulator and a glass wool flow restrictor element were used in conjunction with a Barton differential pressure indicator and a throtting valve. A metal powder feeder

apparatus, which has been described in detail in Reference 12, is used to add the desired amount of aluminum powder to the oxygen gas stream at a constant rate.

Since flash-back of the flame from the tube to the supply system damages the feeder parts, special attention was given to the design of the flow system to minimize the possibility of flash-back. Unfortunately, flash-backs could not be prevented completely since sparks from electrostatic charges were sufficient to ignite the mixture either when the flows were being adjusted or when the detonation tube was being filled. Although the use of dry powder increases the tendency of the flowing heterogeneous mixture to produce static charges, it was necessary to employ dry aluminum powder in the feeder apparatus to assure uniform flow rates. To prevent the flame from reaching the powder feeder mechanism during an experiment, a specially designed knife valve was used to physically separate the detonation tube from the feed system immediately prior to ignition of the mixture.

The concentrations of aluminum powder in the mixtures of the early experiments were determined on the basis of calibrations of the feeder mechanism. The mass flows of aluminum were linear with feeder speed and were initially accurate to within 1 percent of the maximum flow.[12] However, due to wear and warpage of the teflon metering gear, the mass flows would gradually shift. To guarantee more accurate mixtures, the

mass flows were determined prior to or following each experiment. After some experience with this procedure, it was decided to calibrate the flow immediately prior to an experiment.

The various types of ignitors used to initiate combustion of the heterogeneous mixtures included: 1) pressure generating squibs, 2) detonator caps and 3) exploding silver wires. The pressure generating squibs were supplied by the Dupont Manufacturing Company and were of the S-68 variety charged with 3 and 6 grains of powder. The blasting caps were of the No. 6 variety supplied by the Hercules Powder Company. The exploding wire ignitors were made from 0.0045" diameter silver wire and were 3/16" long. All of the above ignitors were initiated electrically with 110 v ac.

The detonation tubes used for these experiments were approximately 9 feet long and were mounted vertically. The powder-gas mixtures entered at the top to give it downward flow. This procedure reduced the problems associated with gravitational effects. Tubes with inside diameters of 19.5 mm, 26.4 mm, 44 mm and 55.2 mm were used. Most of the experiments were conducted with the 26.4 mm diameter size. The induction distance and the detonation wave velocity were determined from photographic records of the flame. Although the glass tubes were shattered by the explosions in the experiments, the results were not affected by the breakage.

Glass tubes with different wall thicknesses were tried, however, none were sufficiently strong to withstand the pressure generated during detonation of the mixtures. Using a nominal wall thickness of approximately 1.2 mm, a well-established heterogeneous detonation wave usually fractured the 26.4 mm tube into very small pieces.

The tubes were wrapped with an army-type cloth adhesive tape except for a narrow region which served as a window (approximately 1/2" wide) facing the camera. To determine whether the shattering glass had any effect on the observed results, a series of experiments were made with the glass tubes surrounded by a heavy metal tube having a window 3/16" wide and 6 feet long facing the camera. A metal tube with an inner diameter of 27 mm was employed for measuring the detonation pressures.

Instrumentation

The propagating flame fronts were photographed with a high-speed strip film camera on Kodak 70 mm Tri-X Film. Synchronization of the camera shutter with the propagating flame front was accomplished by a modified drop-type shutter apparatus which controlled the ignition apparatus.

The pressure behind the high-speed detonation wave was measured with Kistler Model 603-A quartz pressure transducers. The charge on the crystal, produced by the force on the transducers, was amplified and converted to a voltage with

a Kistler Model 566 multirange electrostatic charge amplifier. This signal was subsequently recorded on a Tektronik Model 564 Storage Oscilloscope and a Tekronik Model 555 Dual Beam Oscilloscope. The pressure transducer was mounted flush with the inside wall of the detonation tube and located at a distance approximately 7.5 feet distant from the point of ignition. The long distance between the ignition point and the transducer was necessary to give the detonation wave sufficient distance to stabilize. The manufacturer's static transducer calibrations were used for evaluating the pressure data.

Method

The operational procedure was as follows: (1) Set the strip film camera to the desired speed for measuring the wave velocity. (2) Set first the oxygen-gas flow and then the aluminum powder flow to the desired values with the mixture being exhausted directly to the atmosphere. (3) After the flows were stable, calibrate the powder flow. (4) Flow the test heterogeneous mixture into the detonation tube. (5) After the mixture in the tube was uniform, the synchronizing shutter apparatus was actuated. The latter operation simultaneously separated the feed line and powder feeder apparatus from the detonation tube and ignited the mixture in the tube. The drop shutter exposed the film to the propagating flame while the output signal from the pressure

transducers was used to trigger the oscilloscopes for pressure measurements.

Two basic experimental problems were encountered: (1) it was difficult to produce uniform and reliable aluminum-oxygen mixtures in the detonation tubes and (2) spurious ignitions of the mixtures by stray electrostatic discharges occurred. Uniform and reliable mixtures were obtained with the powder feeder apparatus by frequent cleaning and calibration of the equipment and by employing dry powder. In addition, the velocity of the mixture in the tube had to be maintained above a certain level, otherwise, the powder would tend to collect along the tube walls and produce density variations both along the tube length as well as across the tube diameter. The flowing dry powder tended to accumulate electrostatic charges when flowing in nonconducting tubes. Sparks resulting from these charges occasionally ignited the mixture and the resulting combustion caused extensive damage to the powder feed apparatus. Damage of this type was kept to a minimum by using metal supply lines wherever possible.

The apparatus, instrumentation and evaluation procedures were checked by measuring the detonation properties of a hydrogen-oxygen mixture at 1 atmosphere pressure. The results of these experiments are reported briefly in Appendix II. The results of the detonation velocities

agree well with both theory and other experimental data. Some difficulty, however, was encountered in reading the pressure transducer data because of oscillations which resulted from the natural frequency of the crystal (175,000 cps). It was decided to use an average value of the indicated pressure which had to be extrapolated to the wave front. This procedure yielded pressures for the hydrogen-oxygen mixtures which were approximately 8 percent below the theoretical values obtained on the basis of a Chapmann-Jouquet detonation (Appendix II).

SECTION III

EXPERIMENTAL RESULTS

The experiments were carried out with the mixtures initially at room temperature and atmospheric pressure. The gaseous oxygen used for these studies was an industrial grade supplied by the Liquid Carbonic Company, a Division of General Dynamics Corporation. The manufacturers analysis of this gas is given as minimum oxygen 99.6% plus traces of nitrogen, argon and helium. The actual analysis of the gas in the detonation tube was, however, somewhat different from that given above since some air was aspirated into the system at the junction where the aluminum powder was introduced into the gas stream. This air flow was employed to facilitate the flow of aluminum powder from the feeder apparatus.[12] The amount of air introduced was a function of both the oxygen flow rate and the powder flow rate. The greatest admixture of air occurred when the gas flow rates were high and powder flow rates low. Chromatographic analysis of the gas indicated that the maximum air intake for the normal operational range was less than 0.5 percent of the total volume flow of oxygen. This amount of air increased the nitrogen content to a maximum of 0.3 percent of the total gas. This nitrogen content was considered small and therefore neglected in the theoretical calculations.

Several grades of flake and granular aluminum powders were tried with the result that the finer powders gave more uniform heterogeneous mixtures throughout the detonation tubes. The flake aluminum powder was a pyrotechnic grade (Magna Flake Dark Pyro-Extra Fine) supplied by the Valley Manufacturing Company. Because of the method of manufacture, the impurities in this powder were unknown. The powder is manufactured from sheet aluminum pounded into flake form in a ball mill apparatus. To prevent the flakes from fusing together, stearic acid is used as a lubricant. To remove this acid the powder was thoroughly washed in ethyl alcohol prior to use. While this procedure appeared to remove the bulk of the stearic acid, the purity of the aluminum powder cannot be stated since the treated product was not analysed. The average surface diameter of the flake particles were measured from microphotographs of samples of the powder and found to be approximately 40 microns. The granular powder was grade A-140 supplied by the Aluminum Company of America. It is manufactured from ingots by an atomizing procedure. Composition of the aluminum ingots as given by the manufacturer is: aluminum 99.5%, while maximum values of impurities are iron 0.3%, copper 0.02%, silicon 0.2% and alumina 0.2%. This powder was also analysed by Lyle, Tower and Vruggink[13] who reported an oxide content equivalent to 1.1 percent of the total particle mass. The oxide layer thickness depends

greatly on the temperature and the atmosphere in which the powder is stored. The powder was heated to 95 to 120°K prior to use. It was therefore estimated that the powder used in these studies had an oxide content of 2 percent. The average particle diameter of this powder was given by the manufacturer as 5 microns.

The speed of the mixture down the tube varied with mixture ratio and tube diameter but never exceeded 1 m/sec. The maximum Reynolds number based on the oxygen flow rate was approximately 1200. This value is within the laminar flow regime particularly since Doig and Roper[14] reported that the effect of powder in a gas flow is to dampen the turbulence. The compositions of the mixtures are given as the percent mass of aluminum in the total mass of the mixture.

The flame speeds of the mixtures were obtained by the "tube method" (discussed in Section II of this report). The studies were conducted over a mixture ratio range of 29 to 64 percent fuel. Two different flame front structures were observed to propagate through these mixtures; typical examples of which are shown in Figure 2. The type of flame shown in Figure 2a was always observed for mixtures leaner than 46 percent fuel and occasionally for richer mixtures (when ignited with a pressure generating squib). This type of flame front was also observed in the initiation region when mixtures were ignited by means of an exploding silver

wire. The striations observed at the very front of the flame suggests that initially the individual particles burn possibly in a surface-type reaction. Further behind this front, gas phase reactions become predominant. Another type combustion front observed is that shown in Figure 2b. From similar pictures obtained for carbon monoxide-oxygen mixtures by Campbell and Finch,[38] it can be said that the flame propagates down the tube in a spiral manner. Moreover, the combustion front of this type of flame is very sharp, very intense and probably involves only a gas-phase reaction. Some flames were observed to change speed rapidly when propagating the length of the detonation tube (9 ft). This change could have been due to a very long induction period, nonuniform mixtures in the detonation tube or to an initially over driven condition. The reported flame speeds are for steady states. These flames had constant speeds over a distance of at least 1.5 feet.

Propagation of the lean-type, high-speed flames tended to decrease slowly with distance from the ignitor. Therefore, some scatter of results could be expected. The flame speeds measured for this type of combustion of granular and flake powder-oxygen mixtures and for various tube diameters are tabulated in Table 1 and plotted in Figure 3. This graph indicates that the speed of these flames is dependent on tube diameter as well as on mixture ratio. The presence of a

shock wave preceding the flame front and traveling long distances may be surmised from the photographs of Figure 4 which shows flames of very lean aluminum powder-oxygen mixtures ignited by Dupont S68 pressure generating squibs. The burning of individual particles is seen ahead of the main flame front. It appears possible that ignition occurs as the shock wave passes over the particles. The distance of the burning particle path between the particle ignition point and that of the main flame is interpreted as the separation distance between the shock front and the flame front. The speed of the flame is seen to decrease with distance from the point of ignition. The decrease in flame velocity is caused by expansion waves which diminishes the strength of the shock.

A photograph of a typical rich (48 to 68 percent fuel) aluminum powder-oxygen mixture burning in a 26.4 mm diameter tube and ignited with an exploding silver wire ignitor is given in Figure 5. As seen from this photograph, the mixture burns at its normal rate for a short period after ignition. Thereafter, the flame accelerates slowly (probably due to an increase of the flame burning surface area). For this portion of the combustion, the front of the flame is striated indicating individual particle surface combustion. Thereafter, the flame accelerates very rapidly, probably due to the mixture ahead of the flame becoming turbulent and

also to increasing strength of the shocks preceding the flame. Eventually, some ignition ahead of the main flame occurs after which the flame accelerates very rapidly. Shortly after this rapid acceleration, the front of the flame transforms from the striated appearance to a very intense, sharp wave front. The intensity of the radiation of the flame is seen to decrease rapidly behind the wave front. This decrease is caused by the deposits of oxide on the tube wall. The subsequent intense region thereafter is caused by breakage of the glass tube.

The distance from the point of ignition to that point where the combustion front transforms to a gas-phase reaction and where the velocity first exceeds the Chapman-Jouquet detonation velocity value is called the detonation induction distance. After reaching the high velocity, the flame front takes on a spin appearance. If the mixture had a sufficiently short induction distance, the flame would stabilize. Constant speed of the spinning flame fronts were observed in the 9-foot detonation tubes only in the 26.4 and the 44 mm diameter tubes. The wave lengths of a spin cycle observed in the 26.4 mm diameter tube depended on the type of aluminum powder. For very clean flake powder, the oscillations had nearly the same wave lengths as those of the granular powder-oxygen mixtures, otherwise, they were shorter (corresponding to higher frequencies). The frequency

of the spin of the mixtures burned in larger diameter tubes was lower (wavelengths of the spin cycles were longer). The effect of tube diameter, particle geometry and mixture ratio on the oscillation frequency and wavelength are given in Tables 2 and 3. Figure 6 shows photographs illustrating the effect of tube diameter on the spin wavelength for detonating flake powder-oxygen mixtures.

The average flame velocity as a function of the distance from the point of ignition for the flame shown in Figure 5 is presented in Figure 7. As seen from the latter figure, the flame accelerates slowly at the outset. The speed then increases rapidly until the flame front reaches a peak value. Finally, the flame velocity decreases to a constant average value (the detonation velocity). Detonation velocities for the flake and granular-powder-oxygen mixtures are tabulated in Tables 2 and 3 respectively and plotted in Figure 8. As seen from the graphical representation of the data, the detonation velocities are independent of tube size and are only slightly higher for the granular powder. The lower velocities of the flake powder-oxygen mixtures are believed to result from the impurities. Mixtures richer than 64 percent fuel could not be produced with the apparatus used. The scatter of the data is believed to result from mixture ratio variations as well as from impurities on the powder. The steady detonation speeds for the leaner mixtures are

approximately 1550 m/sec and decrease slowly with mixture ratio.

The induction distances for the various detonateable mixtures ignited by exploding silver wires are also given in Tables 2 and 3 and are plotted in Figure 9. The scatter of these data probably results from the ignition variations and the impurities on the aluminum powder. The induction distances were found to be shorter for richer mixtures and longer for the larger diameter tubes.

A typical record of the pressure behind the detonation wave front as a function of time is given in Figure 10a. As seen from this photograph, the pressure rises very rapidly. The trace has a high frequency oscillation superimposed upon a low frequency oscillation. The high frequency oscillation is that of the natural frequency of the quartz transducer (175,000 cps) and results from the sudden application of the pressure to the transducer. The lower frequency oscillation represents an oscillation of the pressure due to the spinning character of the flame. It is interesting to note that the low frequency pressure oscillations from two diametrically opposed transducers are 180 degrees out of phase (Figure 11). After several damped low frequency pressure oscillations, both transducers yield approximately the same value of pressure (15 cm behind the wave front). This pressure decreases slowly with distance behind the wave

as is shown by the lower sweep rate pressure-time photograph given in Figure 10b (200 microseconds per centimeter). The detonation pressure was taken as the average value behind the first low frequency pressure pulse. Details of the pressure evaluation are presented in more detail in the discussion of the hydrogen-oxygen pressure measurements made to check out the apparatus (Appendix II). The transducer calibration values used in this evaluation were those given by the manufacturer for a static calibration. The results of the detonation pressure measurements are tabulated in Table 4 and plotted in Figure 12 which shows that the measured pressures are approximately 31 atmospheres in the 45 to 60 percent fuel mixture ratio range studied.

SECTION IV

THEORETICAL CALCULATION OF DETONATION PARAMETERS

The detonation parameters of the aluminum powder-oxygen system were calculated according to the methods described in Appendix I. Since the calculations involve the solution of higher degree equations, iteration procedures were employed. The calculations were programmed in Scatran language and executed on the IBM 7094 computing machine at The Ohio State University Numerical Computation Laboratory. The procedure to determine the composition of the species behind the detonation wave front is identical to the method employed in the flame temperature calculations. Therefore, the flame temperature calculation was programmed initially and this basic program was used later as a subroutine in the detonation calculation. Moreover, the results of the temperature calculations could be checked against some previously unpublished aluminum powder-oxygen flame temperature measurements which are discussed in Appendix III.

Since the experimental apparatus and instrumentation was checked with the hydrogen-oxygen system, it was decided to check the general iteration procedures of the computer program by calculating the detonation properties of the hydrogen-oxygen system. The results of this calculation

are reported in Appendix II and were found to agree with previously published calculations.

Flame temperature calculations

Adiabatic flame temperatures are based on the fact that in this case the enthalpy of a given mass of the unreacted mixture is equal to the enthalpy of the same amount of mass of the reacted mixture. Considering a unit mass of the mixture, we can write this condition as

$$\sum_i n_i \Delta H_f^{i,T_1} = \sum_i n_i \Delta H_f^{i,T_2} \qquad (1)$$

where: n_i = specific molality of species i $\left[\frac{\text{moles of i}}{\text{unit mass of mixture}}\right]$.

$\Delta H_f^{i,T}$ = heat of formation of species i at temperature T.

subscripts 1 and 2 refer to the unreacted and the reacted states respectively.

The determination of the flame temperature requires an iteration on the reacted state temperature; and for each temperature an iteration to determine the composition of the reacted state. For known initial conditions (p_1, T_1) and for an estimated value of flame temperature (T_2), the composition of the gaseous species in the reacted state may be calculated according to the procedures described in

References 15 and 16. The accuracy of the assumed flame temperature (T_2) may now be checked by substituting the calculated species concentrations into Equation 1. If the enthalpy difference of the reactants and the products is not within the accuracy desired, then a new reacted state temperature must be assumed and the above steps repeated.

Flame temperature calculations of the aluminum powder-oxygen mixtures (T_1 = 298.16°K, p_1 = 1 atm) were made initially considering only gaseous species in the reaction zone. The two gas species cases considered were Case A: seven gaseous species (O, O_2, Al, Al_2, AlO, Al_2O, Al_2O_2) and Case B: eight gaseous species (O, O_2, Al, Al_2, AlO, Al_2O, Al_2O_2, Al_2O_3). The equations used for the composition calculations of Case A are:

Total pressure:

$$p = p_O + p_{O_2} + p_{Al} + p_{Al_2} + p_{AlO} + p_{Al_2O} + p_{Al_2O_2} \tag{1A}$$

Ratio of elements:

$$\alpha = \frac{N_{Al}}{N_O} = \frac{p_{Al} + 2p_{Al_2} + p_{AlO} + 2p_{Al_2O} + 2p_{Al_2O_2}}{p_O + 2p_{O_2} + p_{AlO} + p_{Al_2O} + 2p_{Al_2O_2}} \tag{2A}$$

Equilibrium:

Chemical Reaction	Equation	
$O_2 \rightleftharpoons 2O$	$K_{O_2} = \frac{p_O^2}{p_{O_2}}$	(3A)
$Al_2 \rightleftharpoons 2Al$	$K_{Al_2} = \frac{p_{Al}^2}{p_{Al_2}}$	(4A)
$AlO \rightleftharpoons Al + O$	$K_{AlO} = \frac{p_{Al} p_O}{p_{AlO}}$	(5A)
$Al_2O \rightleftharpoons AlO + Al$	$K_{Al_2O} = \frac{p_{AlO} p_{Al}}{p_{Al_2O}}$	(6A)
$Al_2O_2 \rightleftharpoons 2AlO$	$K_{Al_2O_2} = \frac{p_{AlO}^2}{p_{Al_2O_2}}$	(7A)

where: p = pressure of mixture.

p_i = pressure of species i in mixture.

N_i = total number of atoms of element i in a given mass of mixture.

n_i = specific molalities of specie i.

K_j = equilibrium constant of reaction j in terms of the respective partial pressures of the species.

Other independent equilibrium equations employing other combinations of species could also have been used. The iteration procedure consisted in estimating the pressure of species i (p_o) in the mixture. The equation for the ratio of

elements was used to check the quality of the estimated value (see References 15 or 16 for details).

The method of flame temperature calculation of Case B (eight gaseous species in the reaction zone) is similar to that of case A. Since for this case another species is present which involves no elements different from those present in the other species, one additional independent equilibrium equation is required. This equation takes the form of an equilibrium equation involving the decomposition and formation of $Al_2O_3(g)$. Moreover, the presence of this additional species will require a modification of the total pressure equation and the ratio of elements equation. The modified and additional equations for the eight species case take the form:

Total pressure:

$$p = p_O + p_{O_2} + p_{Al} + p_{Al_2} + p_{AlO} + p_{Al_2O} + p_{Al_2O_2} + p_{Al_2O_3} \qquad (1B)$$

Ratio of elements:

$$\alpha = \frac{N_{Al}}{N_O} = \frac{p_{Al} + 2p_{Al_2} + p_{AlO} + 2p_{Al_2O} + 2p_{Al_2O_2} + 2p_{Al_2O_3}}{p_O + 2p_{O_2} + p_{AlO} + p_{Al_2O} + 2p_{Al_2O_2} + 3p_{Al_2O_3}} \qquad (2B)$$

Equilibrium:

$$Al_2O_3(g) \rightleftharpoons 2AlO + O \qquad K'_{Al_2O_3} = \frac{p^2_{AlO}\, p_O}{p_{Al_2O_3}} \qquad (3B)$$

The thermodynamic properties of the gas species O, O_2, Al, Al_2, AlO, Al_2O, and Al_2O_2 were taken from NASA Tables[10] while the properties of the gaseous Al_2O_3 species were taken from General Electric Tables.[17] The results of the atmospheric pressure aluminum powder-oxygen flame temperature calculations for the 7 and 8 species cases and based on the dust particles containing 2 percent oxide coating (by mass) are tabulated in Tables 5 and 6 respectively and represented graphically in Figure 13.

Calculations of the adiabatic flame temperatures of the aluminum powder-oxygen system were also made for the case that the species in the reaction zone include in addition to the gaseous species O, O_2, Al, Al_2, AlO, Al_2O, Al_2O_2, the liquid species Al_2O_3. The procedure to calculate the species concentration for this case differs from the method described above since the equilibrium between the liquid species and its gaseous products must be used. Physical chemists generally agree that the molecule Al_2O_3 does not exist in the gaseous state.[18,19] The equations employed in the calculation of the species in the reaction zone for this case (Case C) are:

Total pressure:

$$p = p_O + p_{O_2} + p_{Al} + p_{Al_2} + p_{AlO} + p_{Al_2O} + p_{Al_2O_2} \qquad (1C)$$

Ratio of elements:

$$\alpha = \frac{N_{Al}}{N_O} = \frac{n^g_{Al} + 2n^g_{Al_2} + n^g_{AlO} + 2n^g_{Al_2O} + 2n^g_{Al_2O_2} + 2n^g_{Al_2O_3}}{n^g_O + 2n^g_{O_2} + n^g_{AlO} + n^g_{Al_2O} + 2n^g_{Al_2O_2} + 3n^g_{Al_2O_3}} \quad (2C)$$

Equilibrium:

Reaction	Equation	
$O_2 \rightleftharpoons 2O$	$K_{O_2} = \frac{p_O^2}{p_{O_2}}$	(3C)
$Al \rightleftharpoons 2Al$	$K_{Al_2} = \frac{p_{Al}^2}{p_{Al_2}}$	(4C)
$AlO \rightleftharpoons Al + O$	$K_{AlO} = \frac{p_{Al} p_O}{p_{AlO}}$	(5C)
$Al_2O \rightleftharpoons AlO + Al$	$K_{Al_2O} = \frac{p_{AlO} p_{Al}}{p_{Al_2O}}$	(6C)
$Al_2O_2 \rightleftharpoons 2AlO$	$K_{Al_2O_2} = \frac{p_{AlO}^2}{p_{Al_2O_2}}$	(7C)
$Al_2O_3(liq) \rightleftharpoons 2AlO + O$	$K_{Al_2O_3} = \frac{p_{AlO}^2 p_O}{a_{Al_2O_3}}$	(8C)

where: a_i = activity of species i.

n^g_i = specific molality of species i based on a unit mass of the total gas .

Brewer and Searcy[18] studied the vaporization of Al_2O_3 by means of the Knudsen Effusion cell. From consideration of the observed pressures and the heat of vaporization, the

above authors suggested equilibrium equation (8C) as that reaction involving the liquid alumina. The chemical activities (a) of the species when that species is a perfect gas is identical to the partial pressure of the gas (i.e. $a_i \equiv p_i$). The chemical activity of the liquid species was equated to one.[16,20] For similar calculations, Zeleznik and Gorden[22] also used unit activity for the liquid species. Note that the ratio of elements expression in this system of equations is given in terms of the specific molalities of the gaseous species, the unit mass being that of the total gaseous species only. This set of equations is also solved iteratively, starting by first finding the composition of the gaseous species. Assuming the partial pressure of atomic oxygen (p_o) and substituting into equations (8C), (5C), (3C), (4C), (6C), (7C) in that order, the composition of the gaseous species at a given pressure and estimated temperature may readily be determined. A check of the assumed value can then be made from the total pressure equation (which for the temperature calculation equals the initial pressure). The specific molalities of the gaseous species in the reacted zone (n_i^g) may then be calculated from the following equation:

$$n_i^g = \frac{p_i}{\sum_i m_i p_i} \qquad (2)$$

From the ratio of elements equation (Equation 2C) we may now compute the gas specific molality of the liquid alumina species (Al_2O_3,liq) as follows:

$$n^{g}_{Al_2O_3,liq} = \frac{-\alpha n^{g}_{O} - 2\alpha n^{g}_{O_2} + n^{g}_{Al} + (1-\alpha) n^{g}_{AlO} + (2-\alpha) n^{g}_{Al_2O} + (2-2\alpha) n^{g}_{Al_2O_2}}{(3\alpha - 2)} \quad (3)$$

With the gas specific molalities of all species, the specific molalities of the entire mixture (n_i) may be calculated from the following equation:

$$n_i = \frac{n^{g}_{i}}{1 + 102\, n^{g}_{Al_2O_3,liq}} \quad (4)$$

Having the specific molalities of the combustion products at an estimated flame temperature and for given initial conditions, the correctness of the estimated flame temperature may be checked by substituting into Equation 1. If this equation is not satisfied to the desired accuracy, then a new temperature is estimated and the calculation repeated. In attempting to solve this problem, it was not possible to obtain a solution when the flame temperature was greater than 4005°K for the atmosphere pressure case when the dust particle mass comprised of 98 percent aluminum and 2 percent alumina (solid Al_2O_3). Using a different iteration procedure (Newton Rapson Method) Zeleznic and Gorden[22] developed a program which was used to calculate the flame temperatures of burning pure

aluminum-oxygen mixtures. These authors employed the same basic equilibrium relations as was employed in the present calculation. Their program failed to converge to a composition at 1 atmosphere pressure at a temperature of approximately 4020°K. However, their program gave aluminum-oxygen flame temperatures below this value. In cases where the present program worked the results agreed with those of Gorden and Zeleznic for pure aluminum. Results for the Case C adiabatic flame temperature calculation are tabulated in Table 7 and plotted in Figure 13.

Detonation calculations

The calculation of the detonation wave properties of the aluminum powder-oxygen system followed the general procedures outlined in Appendix I. The only difference between the present system and that discussed in the Appendix is that the mixture is initially heterogeneous and could also be heterogeneous in its final state. The basic equations used in the calculation are:

Detonation wave velocity:

$$u_1^2 = \frac{p_1}{\rho_1} \frac{\left(\frac{p_2}{p_1} - 1\right)}{\left(1 - \frac{\rho_1}{\rho_2}\right)} \qquad (5)$$

Hugoniot equation:

$$\sum_i n_i \Delta H_f^{i,T_2} - \sum_i n_i \Delta H_f^{i,T_1} = \frac{1}{2} \frac{p_1}{\rho_1} \left(\frac{p_2}{p_1} - 1\right)\left(1 + \frac{\rho_1}{\rho_2}\right) \tag{6}$$

Particle velocities behind the wave:

$$u_p = u_1 - u_2 = \sqrt{\frac{p_1}{\rho_1}\left(\frac{p_2}{p_1} - 1\right)\left(1 - \frac{\rho_1}{\rho_2}\right)} \tag{7}$$

Density of unreacted mixture:

$$\rho_1 = \frac{1 + X}{\frac{1 - \text{oxide}}{\rho_{Ae_2O_3}} + \frac{\text{oxide}}{\rho_{Ae}} + X\rho_{O_2}} \tag{8}$$

$$X = \frac{m_{O_2}}{m_{Ae}} = \frac{(1 - \text{oxide})\left(\frac{16}{27}\right) + \text{oxide}\left(\frac{32}{102}\right)}{\alpha} - \text{oxide}\left(\frac{48}{102}\right)$$

Density of reacted mixture:

$$\rho_2 = \frac{\sum n_i {}^*m_i}{V} \tag{9}$$

where: u_1 = detonation velocity = wave velocity of the front of the wave.

u_2 = wave velocity of the rear of the wave.

u_p = particle velocity behind detonation wave.

${}^*m_i$ = molecular weight of species i.

p = pressure.

V = volume per unit mass of total mixture.

ρ = density.

n_i = specific molalities of species i.

m = mass.

$\Delta H_f^{i,T}$ = heats of formation of species i at temperature T.

oxide = percent mass of oxide in dust particle.

$$\alpha = \frac{N_{Al}}{N_O} = \frac{\text{number of Al particles per unit mass of mixture}}{\text{number of O particles per unit mass of mixture}}.$$

Subscripts: 1 = unreacted state.

2 = reacted state.

Although the experiments were conducted with the reactants having an initial velocity of 1 m/sec, the theoretical calculations were carried out for the case that the initial gas was at rest. This assumption has a very small effect on the final results since the detonation wave velocities are much larger than the initial velocity. The solid aluminum and liquid alumina particles were assumed to be small (less than 2 microns) so that no significant relative motion between the different phase particles existed.[23] The system was further assumed to be in thermodynamic and chemical equilibrium. The detonation was considered to be of the Chapman-Jouquet type and the initial conditions of the mixtures were assumed to be 1 atmosphere pressure and 298.16°K temperature. In addition, the gas species were assumed to be perfect gases

and the liquid alumina density constant at 2.7 gm/cc.[21] Detonation parameter calculations were made for the same three product species composition cases considered in the flame temperature calculations. A discussion of the procedure for the calculation of the detonation properties is given in Appendix I. The calculations were made for the case that the dust particle mass was 98 percent aluminum and 2 percent alumina.

Results of the detonation calculations of the aluminum powder-oxygen mixtures are tabulated in Tables 8 through 10 and represented graphically in Figure 8 and 12. Theoretical solution of the Case C combustion products case worked only for the mixture ratios $.9 < \alpha < .6$. The program of Zeleznik and Gorden[22] which used the Newton Rapson iteration method appeared to have the same basic problem. The reasons for the lack of a solution of this system has not been definitely established as yet.

SECTION V

DISCUSSION OF RESULTS

The combustion of the fine aluminum powders with gaseous oxygen at one atmosphere pressure was investigated over the mixture ratio range of 29 to 64 percent powder (by mass). When mixtures leaner than 46 percent fuel were ignited with exploding silver wires, the combustion wave usually accelerated continually over the length of the combustion tube. For these cases, the combustion was shown to be that of a high speed flame. It is possible that in tubes longer than those employed in this study (i.e. longer than 9 feet) a stable detonation condition for some of these mixtures could have been reached. The aluminum powder-oxygen mixtures in the 48 to 68 percent fuel range had induction distances shorter than 6 feet and the propagating wave reached a constant speed. A summary of the important experimental flame properties in this mixture ratio range is given below.

1) Using 26.4 mm diameter combustion tubes and igniting the mixtures with exploding silver wires, the flames accelerated during the induction period to a very high velocity (Figure 7).

2) The detonation induction distances decrease with increasing mixture ratio (Figure 9).

3) The mechanism of combustion in the vicinity of the wave front changes from a combination surface-gas phase reaction in the induction region to a predominately gas-phase reaction thereafter (Figure 5).

4) The wave is overdriven at the onset of detonation (Figure 7).

5) The stabilized flame front is nonplanar and spins as it propagates down the tube (Figure 5).

6) After the flame reaches the detonation induction distance, a shock wave (retonation wave) propagates back into the induction region (Figure 5).

7) The average detonation velocity of the lean mixture flames is approximately 1550 m/sec and decreases with increasing mixture ratio (Figure 8).

8) The pressure behind the stabilized detonation wave fronts is approximately 31 atmospheres over the mixture ratio range studied (Figure 12).

9) Pressures indicated by diametrically opposed pressure transducers yield pressure peaks and troughs that are 180 degrees out of phase (Figure 11).

10) The shape of the aluminum powder and the tube diameter in general have very little effect on the flame velocities and detonation pressure but do affect the induction distances and the spin frequency of the flame.

11) The flame spin parameter is approximately 3.5 for the flake powder and 4.1 for the granular powder (Tables 2 and 3 respectively).

The purpose of this study was first to establish whether heterogeneous aluminum powder-oxygen mixtures are detonable and if so, then to measure the induction distances, the wave velocities and pressure behind the wave fronts. Finally the results would be compared with theoretical values.

Hydrogen-oxygen mixtures were used to check out the apparatus, the instrumentation and the method of data evaluation (Section II). It was quite helpful to compare the strip film photographs of the aluminum powder-oxygen flames to those of hydrogen-oxygen mixtures. Figure 14a is a strip film photograph of a typical hydrogen-oxygen mixture ignited with an exploding silver wire. This photograph shows that the combustion wave accelerates in the induction region and reaches a steady state value after it has been overdriven. A shock wave is also seen to propagate from the point of initiation back into the induction region (a retonation wave). Figure 14b is a strip film photograph of a rich granular aluminum powder-oxygen mixture also ignited with an exploding silver wire ignitor. As seen from this figure, the heterogeneous flame has all the characteristics of that of the hydrogen-oxygen flame; that is, it has an induction period with an accelerating flame, a retonation wave and a

steady state flame velocity value. The one basic difference between the aluminum-oxygen flame photograph and that of the hydrogen-oxygen mixture is that the former propagates in a nonplanar, oscillatory manner after attaining its high speed stable state. The classical example of a detonating mixture with a spinning flame is that of carbon monoxide-oxygen mixtures, first observed by Campbell and Woodhead. The average detonation velocities of the latter mixtures are equal to their theoretical Chapmann-Jouquet values. Lewis and Von Elbe[24] report that near the limits of detonation of all gas mixtures, the flames are of the oscillatory type. Edwards, Williams and Breeze[25] observed oscillatory flames in both rich and lean limits of detonating hydrogen-oxygen mixtures. Details of the oscillating flame of the aluminum-oxygen mixtures will be discussed later.

After the flame reached the induction distance, the high pressure behind the wave caused the glass detonation tubes to shatter into very small pieces. The shattering of the glass occurred just after the flame front had passed by a few centimeters. The observation that the expansion waves resulting from the breakage of the tube had no effect on the wave velocities serves as excellent evidence that the Chapman-Jouquet state behind the wave was established. To support this conclusion, a series of experiments were made in glass tubes surrounded by a heavy metal shell (except for a

3/16-inch slot in the metal tube and facing the camera). The results were found to be identical. In reference to the glass detonation tube, apparently the speed of the combustion products behind the wave was sonic, a condition which would prevent expansion waves from reaching the wave front. The latter is a requirement for a stabilized Chapman-Jouquet detonation wave. Lean aluminum powder-oxygen mixtures which were ignited with pressure generating squibs frequently resulted in very high flame velocities which decreased slowly with distance from the ignition point. Apparently these waves were overdriven and the combustion products behind the wave front were not sonic relative to the front of the wave. Therefore, expansion waves due to cooling of the combusted mixture were able to travel to the wave front and weaken it.

Time histories of the pressure behind the stabilized detonation waves in the aluminum powder-oxygen mixtures indicate that the pressure rises abruptly to very high values (Figure 10). The pressure traces are similar to those of detonating hydrogen-oxygen mixtures (Appendix II) suggesting further that the high-speed aluminum powder-oxygen combustion is that of a detonation. The heterogeneous mixture pressure traces had an additional low frequency oscillation believed to result from the spiraling wave path. Oscillatory flame pressure traces of this type have also been observed for carbon monoxide-oxygen detonations by Mooradian and Gordens.[26]

From the experimental observations of the acceleration of the flame, the generation of a retonation wave, the stabilized high-speed combustion wave, the abrupt rise and the high values of pressure behind the wave front and the similarity of these characteristics to those of known detonating homogeneous gas mixtures, it can be stated that the aluminum powder-oxygen mixtures in the mixture ratio range of 48 to 64 percent fuel are detonable.

Having established that the heterogeneous aluminum powder-oxygen mixtures are detonable, it is desirable to compare the measured detonation properties of the mixtures with their theoretical Chapman-Jouquet values.

The adiabatic flame temperature and combustion gas composition calculation of the aluminum powder-oxygen system validated the detonation composition calculation procedures and provided some insight into the reliability of the thermodynamic properties of the oxides of aluminum. This conclusion is true because the results of the theoretical values compared favorably with the experimental Bunsen-burner flame temperature work for this system which was conducted earlier at this laboratory (Appendix III). The emission spectrum of the aluminum powder-oxygen Bunsen-burner flames showed the presense of O, O_2, Al, AlO species plus traces of impurities.[9] A very intense continuum was also observed, resulting

from the black body radiation of the liquid alumina species. Other aluminum oxide species reported by Brewer and Searcy[18] and Drowart et al[19] in their studies of the vapor pressure and the decomposition of species above liquid alumina were gaseous Al_2O and gaseous Al_2O_2. Gaseous Al_2O_3 has not been detected by investigators and it is generally thought that this species does not exist. In their analysis of the possible reactions which produce liquid alumina (Al_2O_3), Brewer and Searcy indicated that the following equilibrium reactions as most likely.

$$2AlO + O \Longrightarrow Al_2O_3(liq) \qquad (R6)$$

$$Al_2O_2 + O \Longrightarrow Al_2O_3(liq) \qquad (R7)$$

The particular equilibrium reaction used in the theoretical calculation should, however, have no effect on the final answers. Martin, Kydd and Browne[27] in their study of diborane-air (B_2H_6-Air) mixtures found that the lean mixture combustion products consisted only of gaseous products while the rich mixtures contained some liquid B_2O_3. It was therefore decided to calculate the aluminum-oxygen detonation properties also for the case that the products are gaseous. Calculations were made for the following three product species cases (see Section IV for details of calculation)

Case	Gas Species	Liquid Species
"A"	O, O_2, Al, Al_2, AlO, Al_2O, Al_2O_2	
"B"	O, O_2, Al, Al_2, AlO, Al_2O, Al_2O_2, Al_2O_3	
"C"	O, O_2, Al, Al_2, AlO, Al_2O, Al_2O_2	Al_2O_3

Results of the calculations for these cases are tabulated in Tables 8 through 10. The theoretical and experimental detonation wave velocities and detonation pressures are plotted in Figures 8 and 12 respectively. As seen in the above figures, the velocities and pressures for the Case "B" case are approximately 12 and 21 percent above the experimentally determined values. Since the reliability of the thermodynamic properties of the gaseous Al_2O_3 species could not be established and since gaseous Al_2O_3 is generally thought not to exist[18] this case was disregarded. Theoretical calculations of the detonation properties of the aluminum-oxygen system based on Case "A" combustion products (gases only and no gaseous Al_2O_3) gave values which are approximately 10 and 22 percent below the experimental detonation wave velocity and pressure values respectively. Adiabatic flame temperatures of this system were also calculated (Figure 13 and Table 5) and were found to be approximately 27 percent below the experimental values. Since it is unrealistic for the theoretical values to be lower than the experimental values when the calculations were made assuming that the system was

in thermodynamic and chemical equilibrium, the combustion of the system was complete and that the process was adiabatic, the Case "A" calculation is considered not correct. Therefore, liquid alumina must be considered as a product species in the calculation (Case "C"). Although the Chapman-Jouquet detonation properties for the Case "C" product species case could not be calculated over the entire mixture ratio range (see Section IV), the data show that the calculated Chapman-Jouquet detonation velocity and pressure values are approximately 10 and 15 percent respectively above the measured values (Figures 8 and 12). Moreover, the adiabatic flame temperature calculations based on Case "C" product species are only a few percent above the measured values (Figure 13).

Since the calculated detonation velocities and pressures were higher than the measured values for the Case "C" calculation, it is well to review the assumption made for the theoretical calculations and to analyse them with regards to the actual case. The assumptions made were (1) pure propellants, (2) complete combustion, (3) no heat losses from the system and (4) thermodynamic and chemical equilibrium. In addition, it was assumed that the thermodynamic properties of oxides of aluminum as reported by McBride et al[10] are reliable, the gases are perfect and the density of liquid alumina is approximately the same as that reported by Kirshenbaum and Cahill at 2700°K.[21]

The assumption of pure propellants is not valid since stearic acid was used in the manufacture of the flake aluminum powder. This probably accounts for the fact that the granular powder-oxygen mixtures generally had higher experimental detonation velocity values than those of similar flake powder-oxygen mixtures. In addition, for smaller particle sizes, the oxide coating could represent a greater fraction of the total particle mass. The oxide layer thickness on sheet aluminum exposed to air at room temperatures and atmospheric pressures is reported by Gulbranson and Wysong[29] to be 100 Å. At higher temperatures, Keller and Edwards[30] reported that Steinheil measured oxide layer thicknesses up to 1000 Å. Lyle, Tower and Vruggink[13] reported that the granular A-140 powder used in the present studies has an oxide coating amounting to 1.2 percent of the total powder mass. Since the powders were heated to approximately 95 - 120°C for extended periods prior to use, the theoretical calculations were made assuming that the oxide constituted 2 percent of the total particle mass. Additional theoretical detonation calculations showed that if the oxide content of the powder was approximately 23 percent of the total mass of the powder, then the theoretical Chapman-Jouquet detonation values would agree approximately with the measured values. Considering the surface area of the granular particles, this oxide layer would correspond to a

thickness of about 600 Å. According to Gulbranson and Wysong, a temperature of 450°C is required to form a layer of this thickness. Since the temperatures at which the powder was prepared for use was considerably below this value and since ignition of the particles would be very difficult with such thick oxide layers, the possibility of the oxide layer causing the difference between theoretical and experimental values is discounted.

The assumption of complete combustion is believed to be relatively good since the temperatures behind the detonation front are above the melting temperature of aluminum (for p = 1 atm, T_{MELT} = 932°K, T_{BOIL} = 2700°K while T_{FLAME} > 4000°K).[45] Of course, some of the larger sized particles, particularly those near the wall of the detonation tube, may not have sufficient time to combust because of quenching effects. The high heat transfer rates to the particles result primarily from the surface reaction and radiation from the flame. The radiation is believed important because of the high intensity of the normal flames[8,9] and also because of the close proximity of the aluminum particles to the flame zone. Grosse and Conway[9] have reported that up to 70 percent of the chemical energy in the aluminum powder-oxygen flame is lost through radiation. From photographs of the detonating mixtures and the microfine dust observed after an experiment, the mechanism of the

aluminum combustion in the detonation process is believed to occur in the gas phase. The assumption of complete combustion is therefore generally thought to be valid.

The assumption of no losses of heat during the detonation is considered to be good. Heat losses would occur primarily through convective and radiative processes. The convective losses are probably of second order because of the relatively small wave thickness and the high flame speeds. Since the radiation emitted from the aluminum-oxygen flame is very high, it would appear then that radiative heat losses may be significant. However, because of the heterogeneous nature of both the reactants and the products, the radiation mean free path is very small thus the losses could also be expected to be small. Moreover, if the radiation losses were significant, then a greater discrepancy between the theoretical and measured flame temperature values could be expected than has been observed.

The assumptions of thermodynamic and chemical equilibrium are good for the hydrogen-oxygen system (see Appendix III). For the aluminum powder-oxygen system, the measured detonation wave velocities are much lower and the waves thicknesses appear greater than those of the hydrogen-oxygen system, therefore, more time is available for processes to occur. Hence, the assumption of thermodynamic equilibrium is probably good. The assumption of chemical equilibrium for

the heterogeneous system is questionable because of the necessity to vaporize the solid aluminum and then to form the condensed alumina species. The most likely chemical reactions in the overall process of the Case "C" situation are the following:

$$Al(solid) \Longrightarrow Al \quad \text{(R1)}$$

$$O_2 \Longrightarrow O + O \quad \text{(R2)}$$

$$Al + O \Longrightarrow AlO \quad \text{(R3)}$$

$$Al + O_2 \Longrightarrow AlO + O \quad \text{(R4)}$$

$$2AlO \Longrightarrow Al_2O_2 \quad \text{(R5)}$$

$$2AlO + O \Longrightarrow Al_2O_3\ (liq.) \quad \text{(R6)}$$

$$Al_2O_2 + O \Longrightarrow Al_2O_3\ (liq) \quad \text{(R7)}$$

$$AlO + Al \Longrightarrow Al_2O \quad \text{(R8)}$$

$$Al_2O + O \Longrightarrow Al_2O_2 \quad \text{(R9)}$$

$$Al_2O + O_2 \Longrightarrow Al_2O_2 + O \quad \text{(R10)}$$

$$2Al \Longrightarrow Al_2 \quad \text{(R11)}$$

$$2AlO \Longrightarrow Al_2O + O \quad \text{(R12)}$$

While all of these chemical reactions may appear in the combustion process of aluminum with oxygen, reactions (R1)

through (R6) would appear more often for lean mixtures while reactions (R1) through (R5) and (R7) through (R12) would appear more often for the rich mixtures. This conclusion is based on the theoretical calculations (Table 10) wherein the dominant gas product species for lean mixtures is AlO while for richer mixtures the dominant gas product species is Al_2O. Brewer and Searcy[18] and Drowart et al[19] also reported the same corresponding dominance of these species experimentally. The chain branching chemical reactions producing active radicals, (R1) through (R4), are common to both rich and lean mixtures. While the theoretical calculations for the 8 species case is based on 6 independent equilibrium relations, certain of the above chemical reactions are more likely to occur than others. For lean mixtures, liquid alumina is probably formed more often through reaction (R6) (because of the abundance of O and AlO species). Brewer and Searcy suggested this reaction as the most likely one to produce the liquid alumina. The Al_2O_2 species was not detected in the spectroscopic analysis of the aluminum-oxygen Bunsen-burner flames[9] and has been found in only very small amounts above boiling alumina by Brewer and Searcy. Therefore, reaction (R7) probably does not contribute significantly to the formation of alumina. Reaction (R6) is a tri-molecular reaction, requiring simultaneous collision of 3 molecules in the proper orientation. For usual 3-body

collisions, the rate of disappearance of 2AlO (corresponding rate of formation of $Al_2O_3(liq)$) is given by the rate equation

$$\frac{d(Al_2O_3)}{dt} = -2 k_3 (AlO)^2 (O) \qquad (10)$$

where: (AlO) = AlO species concentration (moles/cc)

(O) = O species concentration (moles/cc)

t = time

k_3 = three-body rate coefficient.

Barth[46] reported rate constants for ideal three-body collisions as approximately $1.088 \times 10^{15} (\frac{cc}{mol})^2 \frac{1}{sec}$. Using this rate coefficient and the initial concentration as that of the 7-gas specie case (Table 8), the time to form half the alumina species (the half time, $t_{1/2}$) is approximately 37 microseconds. From the pressure and the streak photograph traces, the wave thickness of the process is approximately 3 cm (20 microseconds). In view of the fact that the rate constant used in the above calculation is that for the O_2 or N_2 formation from their elements (in collision with a third body) and that this reaction apparently requires no preferred collision orientation, the present reaction (R6) would have a steric factor which would give longer half times. Moreover, the reaction forms liquid alumina (Al_2O_3) and probably requires that the reaction occur on the surface of a liquid particle. Hence, reaction (R6) would probably require even

more time thus making it even less likely that a state of chemical equilibrium is reached, particularly for rich mixtures. Hence, in all probability, the system is not in chemical equilibrium.

In summary, the assumptions made in the theoretical detonation calculation would tend to give values which are higher than experimental values. The assumptions of pure propellants, complete combustion, perfect gases and heat losses represent minimal effects while the assumption of chemical equilibrium, at least with regards to the liquid alumina species production, would constitute a major deviation from the real case.

As seen from Figure 8 and 12, the theoretical values of velocity and pressure values are approximately 10 and 15 percent respectively above the experimental values. If chemical reaction (R6) is not in equilibrium, the value of equilibrium constant may be altered to compensate for this deviation. Recall that the chemical equilibrium equation of reaction (R6) can be written as

$$Al_2O_3 \underset{r_R}{\overset{r_F}{\rightleftharpoons}} 2AlO + O \qquad (11)$$

where: r_F = forward reaction rate

r_R = reverse reaction rate

The equilibrium constants for this reaction can be expressed as:

$$K = \frac{k_F}{k_R} \tag{12}$$

where: k = rate constant.

In the event that this reaction is not in chemical equilibrium, the constant given by the above equation would be greater than that of the equilibrium value. Because of the variation in temperature, pressure and composition with mixture ratio, it is expected that the nonequilibrium factor would change somewhat with mixture ratio. When a nonequilibrium factor of .002 was applied to the lean mixtures, the theoretical values approximated to the experimental values. This value corresponds to a rate constant $\frac{1}{500}$th of the rate constant used in the above half time calculation. This low rate constant suggests that the liquid Al_2O_3 species has very little chance of attaining its equilibrium composition value before the apparent end of the wave and is probably responsible for the low experimental detonation values.

From the similarities of the strip film photographs of the induction regions of the aluminum powder-oxygen and hydrogen-oxygen systems (Figure 14), it is concluded that the mechanism of detonation initiation of the two systems is

similar. The Becker model of shock wave generation[1] can be used to describe the initiation of heterogeneous detonations. After ignition, the flame burns normally until the flame fills the tube. Because of friction and cooling at the tube wall, the flame surface area increases causing the flame to be accelerated. The increased combustion rate causes pressure waves to be transmitted into the unreacted media. Initially, the waves travel much faster than the flame and, therefore, separate from it. Successive waves travel faster than those preceding them since they are traveling in a region of higher temperature and travel with respect to a gas that has a velocity in the direction of the preceding wave. The result being that the pressure waves will eventually overtake one another forming a shock wave. As the shock wave increases in strength, the gas velocity behind the wave increases, and eventually the flame becomes turbulent. At this stage of induction, several models have been proposed. Martin and White[31] have suggested that the flame accelerates very rapidly along the tube walls. Bone, Frazer and Wheeler[32] proposed that the mixture between the flame and the shock wave autoignites. Oppenheim et al[33] and later Laughrey, Bollinger and Edse[34] have observed ignition ahead of the main flame along the walls of the tube. Strip film photographs of the detonation induction region of carbon monoxide-oxygen mixtures taken by Bone, Frazer and Wheeler

look remarkably similar to those observed for the heterogeneous detonations. For the present studies, autoignition was frequently observed ahead of the main flame, probably at the wall of the tube.

The induction distances of the flake and granular powder-oxygen mixtures are shown graphically in Figure 9. The scatter of the data is believed to result from variation of preparation of the aluminum powder and/or variations of the exploding wire ignitors. Ignitor variations could have resulted from partial shorting of the electrodes due to deposit of metal powder at the base of the electrodes. Variations of the flake powder purity resulted from possible insufficient cleaning. When flake powders were heated to 120°C prior to use, the induction distances were shorter than when heated to 95°C. The induction distances of granular powder-oxygen mixtures were generally longer than those of flake powder-oxygen mixtures. The induction distances decreased with increasing fuel concentration. According to Fong, Bollinger and Edse,[35] the induction distance of homogeneous gas systems is inversly proportional to the burning velocities and the energy released in the chemical reaction and directly proportional to the sound speed. Systems with high burning velocities, low sound speeds and high energy release rates per unit mass of the mixture will tend to detonate easily. The normal flame velocities of aluminum

powder-gas (70 percent oxygen, 30 percent nitrogen) mixtures in combustion tubes was found by Cassell et al[7] to be approximately 40 cm/sec. Using Bunsen-burner flames (Appendix III), normal burning velocities of approximately 25 cm/sec were measured for the aluminum powder oxygen system. For such low burning rates, it would appear very difficult to detonate such mixtures even with the large amounts of heat released in the chemical reaction. Gouse and Browne[28] derived expressions for the isentropic velocity of sound in two-component, two-phase systems. The expression they give for a perfect gas-incompressible solid is

$$\frac{c_m^2}{c_g^2} = \frac{\left(\frac{\rho_g}{\rho_s} + N\right)^2}{N(1+N)} \cdot \frac{\left(\frac{C_{v,s}}{\gamma_g C_{v,g}} + N\right)}{\left(\frac{C_{v,s}}{C_{v,g}} + N\right)} \qquad (13)$$

where: c = velocity of sound

ρ = density

C_v = specific heat at constant volume

γ = ratio of specific heats

m = mass

$N = \frac{m_g}{m_s}$

Subscripts: g = gas

m = mixture

s = solid

This equation shows that the sound speed in a heterogeneous mixture is less than that of the gas alone and for increasing powder density (mass ratio) the mixture sound speed decreases even more. Therefore, the shock wave build-up will be more rapid and the induction distances short for richer mixtures. This agrees with experiment (Figure 9). Dobbins and Tempkin[36] studied the attenuation of sound waves in two-phase media. Their results show that viscous and thermal dissipations are independent of pressure, increase with particle size and that there is an optimum particle size for acoustical impedance. The acoustical impedances are most important for long induction distance, high acoustical velocity systems. Carrier[37] studied the passage of shock waves through dusty mixtures. The result of his study showed that the shock thickness is increased for larger sized and larger mass particles. In the heterogeneous detonation process, it is difficult to assess the particle effect on the shock wave since chemical reactions on the particle surface will occur very rapidly because of the high pressure and high temperature of the oxygen behind the shock wave.

After the induction period and a short overdriven condition, the flame front of these mixtures propagates down the tube in a spiral manner (Figure 5). The average velocity of the flame for a given rich mixture is constant

as seen from the plot of velocity versus a distance (Figure 7). A helical pattern was deposited on the inside wall of the metal tubes during detonation of the rich mixtures. This pattern corresponded to the propagation of a rotating combustion head along the perifery of the tube. The pressure-time traces of detonating aluminum powder-oxygen mixtures were also shown to be oscillatory (Figures 10 and 11). The flame oscillation frequency (or wavelength since the flame speed is almost constant) for a given powder-oxygen mixture was found to be relatively independent of mixture ratio. Flake powders which were not washed prior to use had shorter spin wavelengths (higher frequencies). The frequencies of oscillations in the 26.4 mm diameter detonation tubes were approximately the same for both the granular and very clean flake mixtures. The wavelengths and frequencies of flame oscillations for detonating aluminum powder-oxygen mixtures given in Tables 2 and 3 are summarized below.

Powder	Tube Dia. (mm)	Wavelength λ (cm)	Frequency (1/sec)	$\frac{\lambda}{\text{dia}}$
Flake (uncleaned)	26.4	9.0	16200	3.41
Flake (uncleaned)	44.0	15.2	9700	3.45
Granular	26.4	10.8	14300	4.09

The oscillatory flame front observed in the detonation of the

aluminum powder-oxygen mixtures is not unique to this system. Campbell and Woodhead first observed this phenomena in detonating carbon monoxide-oxygen mixtures. Later, Campbell and Finch[38] established from head-on (axial) photographs that the oscillations resulted from a helically traveling flame head. The head of the flame propagated in a spiral fashion down the tube. Bone, Frazer and Wheeler[32] observed higher spin frequencies when small amounts of hydrogen were added to carbon monoxide-oxygen mixtures. The higher frequencies are the result of increased reaction rates of the system. The higher frequencies observed for the uncleaned flake powder-oxygen mixtures over the cleaned powders may be related to increased reaction rates or greater sound speeds behind the wave as a result of the stearic acid on the powder. Spinning detonations can be either single or multiple headed structure,[38] the multiple structured cases occuring in large diameter tubes. The phenomena of spin detonation and its relation to transverse pressure waves behind the shock fronts of homogeneous gas mixtures was studied first by Manson and later by Fay.[39] Using a rotating wave solution to Raleighs potential equation for the natural vibrations in a cylindrical duct and solving for the approximate boundary conditions, Fay showed that for the lowest mode, the spin pitch (λ) divided by the tube diameter (dia.) is given by

$$\frac{\lambda}{dia} = \frac{\pi u_1}{1.841 c} \qquad (14)$$

The detonation velocity (u_1) divided by the speed of sound (c) at the Chapman-Jouquet point is, to a first approximation, given by

$$\frac{u_1}{c} \approx \frac{\gamma+1}{\gamma} \tag{15}$$

where γ is the ratio of specific heats at the C-J point. For a value of $\gamma = 1.2$, it is found that

$$\frac{\lambda}{dia} = 3.13 \tag{16}$$

This spin detonation parameter agreed remarkably well with the experimental values for the carbon monoxide-oxygen system observed by Bone, Frazer and Wheeler.[32] Barrere[40] derived an analytical expression for the high frequency combustion oscillations observed in small length to diameter ratio rocket combustion chambers ($\frac{l}{dia} < 3$). The oscillation frequency (f) is given by,

$$f = 586 / \frac{c}{dia} \tag{17}$$

where: c = sound speed.

dia = chamber diameter.

This frequency expression corresponds to that obtained for the first tangential acoustical mode[40] and also the first rotary acoustical mode.[39] Berman and Cheney[41] have showed that the high frequency combustion oscillations in rocket

motors (screaming) are of the rotary-type. The pressure traces from opposed transducers and the streak photographs observed in the present studies are very similar to those observed in corresponding studies of the carbon monoxide-oxygen detonations by Mooradian and Gorden[26] and Bone, Frazer and Wheeler[32] respectively.

Detonations with oscillatory combustion are characteristic of systems having low chemical reaction rates or in the detonation limits of other systems. For the latter systems, the chemical energy per unit mass of the mixture is lower resulting in lower temperatures and slower chemical reaction rates. Systems with low reaction rates generally have thicker wave fronts. Transverse pressure waves from the combustion region can, in such systems, build up nodal points. These points would depend on the vessel geometry (tube diameter) and the acoustical properties of the media. The nodal points would have higher pressures and higher temperatures and thus have higher chemical reaction rates. The combustion front would therefore follow the high-pressure nodal point.

The speed of sound in the gas behind a normal shock of velocity equal to that of the detonating aluminum powder-oxygen mixtures (speed = 1550 m/sec) is calculated to be approximately 680 m/sec. The pitch-diameter ratio for a rotating transverse pressure wave for this situation is

given by Equation 17 as 4.0; approximately the same as that observed for this system (Table 3). The frequency as given by the empirical expression for screaming oscillations of rocket motors (Equation 20) is 16000 cycles per second; approximately the same as that observed for this system. It should be remarked that in the above calculation of the sound speed and shock property calculation, the solid particles were not taken into account.

SECTION VI

SUMMARY

It has been shown that fine aluminum powder-oxygen mixtures are detonable. The range of detonable mixtures for the 9-foot long, 26.4 mm diameter combustion tubes is 48 to 64 percent fuel (by mass). The energy required to initiate burning of these mixtures was found to be very small. In some instances, the mixtures were ignited by sparks from the discharge of static charges built-up on the mixture. The detonation induction distances in this mixture ratio range are less than 1.6 meters in length and were found to decrease rapidly for the richer mixtures. This relatively small induction distance is attributed to the low sound speed of the system and the very intense radiation emitted by the flame.

The streak photographs of the flame fronts are similar to those of hydrogen-oxygen mixtures and identical to those of the carbon monoxide-oxygen mixtures. The photographs show a rapidly accelerating flame in the induction region, a retonation wave at the point of initiation of detonation, a flame velocity that is initially overdriven and a spinning flame front during detonation. The pressure behind the wave

front rises rapidly to a very high value. All of the latter characteristics are typical of a detonation wave.

The detonation velocities of this system over the mixture ratio range of 49 - 64 percent aluminum were found to be approximately 1550 m/sec for the lean mixtures and decrease with increasing mixture ratio. The detonation pressures corresponding to this mixture range were found to be approximately at 31 atm. The theoretical values are approximately 10 and 15 percent, respectively, above the measured detonation values. The combustion product species for the calculation were: O, O_2, Al, Al_2, AlO, Al_2O, Al_2O_2 in the gas state and Al_2O_3 in the liquid state. From an analysis of the assumptions made for the calculation, the discrepancy between the theoretical and experimental values are attributed to chemical non-equilibrium. The non-equilibrium results basically from the slow reaction producing the liquid specie since it is a tri-molecular reaction.

The frequency of spin of the flame front of the detonating mixtures results from the buildup of transverse pressure waves in zone between the shock front and the flame front. The aluminum powder-oxygen system has a characteristic flame spin parameter of approximately 4 for the clean powders.

APPENDIX I

METHOD OF DETONATION PARAMETER CALCULATION

The method of calculation of the theoretical detonation properties of explosive mixtures follows the general procedures described by Edse and Fishburne.[15] The assumptions made for this calculation are:

1) One-dimensional wave motion.
2) Thermodynamic and chemical equilibrium.
3) Adiabatic flow.
4) Perfect gases.
5) No relative motion between particles of different phases (implies that if liquid and/or solid particles are present, they are small so that velocities of all particles are the same. This condition generally holds true if particle sizes are less than 2 microns).[23]
6) Chapman-Jouquet condition for stable detonation.
7) No external body forces.
8) Initial conditions:
   a) Mixture is uniform throughout.
   b) No mass motion.
   c) Initial temperature = 298.16°K.
   d) Initial pressure = 1 atm.

Figure 15a is a sketch of an ideal one-dimensional detonation wave. Zone 1 of this figure represents the initial or unreacted state while zone 2 represents the final or reacted state behind the detonation wave. The problem is solved most easily by considering the wave front to be stationary and particles of the system moving relative to it (Figure 15b). Hence, the unreacted mixture in the stationary wave frame coordinates will have a motion to the left into the detonation wave front equal to that of the detonation wave velocity (u_1). The burned particles leaving the combustion zone will also have a motion to the left but will have a speed (u_2) different than the particles entering the wave front because of the different properties after the wave.

The conservation equations for an adiabatic, constant area, stationary coordinate system are as follows:

Mass: $$\rho_1 u_1 = \rho_2 u_2 \qquad \text{(A-1)}$$

Momentum: $$p_1 + \rho_1 u_1^2 = p_2 + \rho_2 u_2^2 \qquad \text{(A-2)}$$

Energy: $$h_1 + \frac{u_1^2}{2} = h_2 + \frac{u_2^2}{2} \qquad \text{(A-3)}$$

where: p = pressure

ρ = density

u = wave velocity

h = enthalpy

Subscripts: 1 = reactants

2 = products

For the case that the reactants or the products are perfect gases, the perfect gas law may be employed and is given by:

$$p\nu = \frac{p}{\rho} = \frac{RT}{\mathcal{M}} \tag{A-4}$$

where: ν = specific volume

R = universal gas constant

$\mathcal{M}$ = molecular weight of gas

T = temperature

ρ = density

An expression for the wave velocity of the reactants (u_1) in terms of pressure ratio ($\frac{p_2}{p_1}$) and density ratio ($\frac{\rho_1}{\rho_2}$) may be obtained from the mass and the momentum equations (Equations A-1 and A-2) and takes the form

$$u_1^2 = \frac{p_1}{\rho_1} \cdot \frac{\left(\frac{p_2}{p_1} - 1\right)}{\left(1 - \frac{\rho_1}{\rho_2}\right)} \tag{A-5}$$

The wave velocity of the products (u_2) may be computed in a similar fashion with the result

$$u_2^2 = \frac{p_2}{\rho_2} \cdot \frac{\left(1 - \frac{p_1}{p_2}\right)}{\left(\frac{\rho_2}{\rho_1} - 1\right)} \tag{A-6}$$

For a stabilized detonation wave, the velocity of the particles in the reaction zone relative to the laboratory system (u_p) plus the velocity of the wave in the reaction zone (u_2) must equal the velocity of the wave in the unreacted zone or

$$u_2 + u_p = u_1 \tag{A-7}$$

The velocity of the particles in the reaction zone can therefore be written as:

$$u_p = \sqrt{\frac{p_1}{\rho_1}\left(\frac{p_2}{p_1} - 1\right)\left(1 - \frac{\rho_1}{\rho_2}\right)} \tag{A-8}$$

Hence, the detonation wave velocity (u_1) and the particle velocity behind the wave (u_p) may be computed for a given system when the pressure and density ratios across the wave are known. An expression relating the density and pressure ratios without the presence of the wave velocities may be obtained by substituting the expressions for u_1 and u_2 (Equations A-5 and A-6) into the energy equation (Equation A-3) and takes the form

$$h_2 - h_1 = \frac{1}{2}\,\frac{p_1}{\rho_1}\left(\frac{p_2}{p_1} - 1\right)\left(1 + \frac{\rho_1}{\rho_2}\right) \tag{A-9}$$

This expression is known as the Hugoniot equation and gives a relationship between the pressure and density ratios and

the enthalpy change across the wave. Since chemical reactions occur in the reacted zone, it is necessary to determine the composition as well as the state of the media behind the wave front. The procedure to calculate the composition of a reacting mixture at a specified temperature and pressure for the condition of chemical thermodynamic equilibrium is discussed in References 15 and 16. With knowledge of the composition of the mixture before and after the wave for a given initial and an estimated final temperature and pressure, the enthalpy difference ($h_2 - h_1$) for a unit mass of the mixture may be obtained as follows:

$$h_2 - h_1 = \sum_i n_i \Delta H_f^{i,T_2} - \sum_i n_i \Delta H_f^{i,T_1} \qquad \text{(A-10)}$$

where: n_i = specific molality of specie i at temperature T.

$\Delta H_f^{i,T}$ = heat of formation of specie i at temperature T.

i = 1, 2..., $\bar{s}$; where $\bar{s}$ = total number of species present in mixture.

The Hugoniot equation may now be written as

$$\sum_i n_i \Delta H_f^{i,T_2} - \sum_i n_i \Delta H_f^{i,T_1} = \frac{1}{2} \frac{p_1}{\rho_1} \left(\frac{p_2}{p_1} - 1\right)\left(1 + \frac{\rho_1}{\rho_2}\right) \qquad \text{(A-11)}$$

For given initial conditions and estimated final pressure, there is one temperature (and corresponding density) which satisfies Equation A-11. A locus of points satisfying the Hugoniot equation may then be determined for a given system at given initial conditions; a plot of which is called the Hugoniot curve of that system. A typical Hugoniot curve is shown plotted in Figure 16.

According to Equation A-5, for each straight line drawn from the initial conditions ($\frac{P_2}{P_1} = \frac{\rho_1}{\rho_2} = 1$) to some point on the Hugoniot curve, there corresponds a detonation wave velocity value. This straight line can be shown to be that of a Raleigh line.[15] The slopping nature of the Hugoniot curve results in the Raleigh lines normally intersecting this curve at two points. The high pressure point (point A of Figure 18) corresponds to that of a subsonic particle flow condition behind the wave while the lower pressure point (point B of Figure 18) corresponds to a supersonic particle flow condition behind the wave. Since the flow behind a normal shock is subsonic, the lower pressure intersection point is disregarded. Because the high pressure intersection point has subsonic flow behind the wave, expansion waves (due to cooling that occurs after passage of the wave) can propagate up to the wave front. These waves reduce the strength of the shock wave and also the wave speed. The original condition considered therefore

was an overdriven case. The effect of expansion waves on the wave on the overdriven condition is to produce a condition of higher Mach numbers behind the wave. As the wave strength is reduced further, as a result of additional expansion waves, a condition is reached wherein it can be shown that the detonation velocity is a minimum (point C on the Hugoniot curve, Figure 16), the entropy is a maximum and the particle Mach number behind the wave is exactly equal to one.[15] For this condition, the effects of cooling behind the wave do not affect the wave. This is the well-known Chapman-Jouquet criterion for a stable detonation. This point corresponds to the tangent point of the Raleigh line with the Hugoniot curve.

APPENDIX II

HYDROGEN-OXYGEN DETONATION PROPERTIES

The theoretical and experimental detonation properties of the homogeneous gas hydrogen-oxygen mixtures were studied for the purpose of checking both the operation of the heterogeneous mixture experimental apparatus and the calculation procedures employed in the heterogeneous detonation computer program. This particular system was selected because it is a simple system and has been studied previously.

The theoretical detonation calculation procedures are discussed briefly in Appendix I and in detail in Reference 15. The basic assumptions made for this calculations include: the system is in thermal and chemical equilibrium, both reactants and products are perfect gases, and the process is adiabatic, the reactants are initially at standard conditions ($T = 298.16^{o}K$, $p = 1$ atm), the detonation is of the Chapman-Jouquet type and the system is initially static. The calculations for this system were made on an IBM 7094 computing machine using the basic program setup for the calculation of the aluminum powder-oxygen detonation properties (Section III). It was only necessary to change the composition equations and the thermodynamic properties of the program to accommodate the hydrogen-oxygen system. The

thermodynamic properties for species used in this calculation were taken from NASA tables[10] and from JANAF tables.[11] The results of these calculations are tabulated in Table 11 and plotted in Figures 17 and 18. These values were found to agree with the values reported previously by Bollinger and Edse,[42] and Edwards, Williams and Breeze.[25] The latter authors used a general program which was setup by Zeleznik and Gorden.[22]

The apparatus used to measure the detonation wave velocities and detonation pressures of the hydrogen-oxygen mixtures was very similar to that used for the aluminum powder-oxygen studies (see Section II). The only difference was that the gases were mixed in an impingement-type mixing chamber and the mixture was initially static. The bulk of the experiments were made in heavy wall 26.4 mm inside diameter glass tubes. Some thin-walled glass tubes were used to determine whether tube breakage had any affect on the measured wave velocity and pressure values. The velocity and pressure values of the stabilized waves were found to be uneffected by the shattering tubes.

Figure 19 shows a typical strip film photograph of a 44.6 percent hydrogen-oxygen mixture (by volume). The results of the detonation wave velocity measurements of this system are tabulated in Table 12 and plotted in Figure 17.

These results agree favorably with those reported by Bollinger and Edse.[43] Compared to the theoretical Chapman-Jouquet wave velocity values, also plotted in Figure 17, the measured values are in very good agreement.

The detonation pressure measurements of this system were made with detonation tubes of heavy wall glass or metal in order to avoid tube breakage. Because of the high cost of the pressure transducer, care was taken to protect it from damage by the detonations. Previous experiments indicated that no significant damage to the transducer occurred when it was subjected to a hydrogen-oxygen detonation. However, because the aluminum powder-oxygen flame is very intense and because of the possibility of powder burning on the transducer surface, it was protected by a thin plastic shield. The shield had no effect on either the transducer operation or the results for the hydrogen-oxygen system. A typical photograph of the pressure traces for the present system is shown in Figure 20. The high frequency oscillation of the output is a result of the natural frequency of the crystal (175000 cps) which is excited by the sudden application of pressure. The interpretation of the data was questionable since the manufacturer calibrated the transducer by applying a static pressure with a dead weight tester apparatus. The present data was evaluated using the manufacturers calibration and the average value of the

oscillations extrapolated to the front of the trace. The results of the detonation pressure measurements are tabulated in Table 12 and plotted along with the theoretical values in Figure 18. These results are seen to be approximately 8 percent below the Chapman-Jouquet pressure values. The experimental values compare favorably with the measurements of Edwards, Williams and Breeze.[25]

Based on the relatively good agreement between the present values (experimental and theoretical) with those reported earlier, it can be stated that the general procedures employed in the detonation investigations are correct.

APPENDIX III

STUDIES OF ALUMINUM POWDER-OXYGEN BUNSEN-BURNER FLAMES

An experimental study of the properties of aluminum powder-oxygen Bunsen-burner flames preceeded the detonation property investigation. This work was sponsored in part by the Hercules Powder Company, Allegany Ballistics Laboratory, Cumberland, Maryland through a contract with The Ohio State University Research Foundation. The apparatus and method used to produce the Bunsen-burner flames is reported in a paper on the emission spectra of these flames.[9] Also studied, but heretofore unreported, were the flame temperatures and burning velocities of the system. Several different spectroscopic procedures for determining the flame temperature from the emission spectrum of the flame were tried. The most reliable temperature data was obtained from the intensity distribution of line spectra. While several different line spectrum were present in the radiation emitted by the flame, best results were obtained from the FeI lines since they appear in a region of low flame continuum and away from other discrete spectrum. The spectrum of the flames were recorded photographically with a 21-foot Jarrel Ash grating spectrograph employing a Wadsworth mounting. The 4-inch-diameter concave grating of

this spectrograph has 1500 lines per inch and gives a reciprocal linear dispersion of 5.0 Å per mm in the first order. Kodak III-F spectroscopic plates were employed for this study. The plates were calibrated with a mercury lamp. The aluminum powder was grade #123 purchased from the Aluminum Company of America Inc. The flames were stabilized on burners having an inside diameter of .95 cm. The spectrum was taken from the emission of the flame at a point immediately above the tip of the flame cone. The iron line spectrum results from a small amount of iron impurities in the aluminum powder. Approximately 40 lines appeared in the wavelength region from 3000 Å to 4000 Å. The electronic temperature was determined by the line slope method.[44]

Results of the temperature measurement of several different mixture ratio aluminum powder-oxygen flames are tabulated in Table 13 and plotted in Figure 13. As seen from this plot, the maximum flame temperature is approximately 3800°K. This result agrees with the suggestion of Grosse and Conway[8] that the maximum temperature of a metal flame is limited by the boiling point of the condensed combustion products. The condensed species of this flame is alumina (Al_2O_3) which has a boiling point of 3800°K at atmospheric pressure.[45] Theoretical adiabatic flame temperature calculations of this system are discussed in Section IV of

this paper. Results of the calculations for the case that the products contain liquid alumina are tabulated in Table 12 and plotted along with the experimental data in Figure 13. The measured values are approximately 5 percent below the theoretical values.

The burning velocities of this system were also determined from the Bunsen-burner flames. Evaluation of these data were made from the flame cone surface area and the unburned volume flow of the mixture. Results of these measurements are tabulated in Table 14 and plotted in Figure 21. The average burning velocity is approximately 25 cm/sec. This value of burning velocity is low for a system having such high heats of combustion (400400 cal/mole). It suggests that the overall chemical reaction is very slow; probably due to surface reactions in the mechanism.

REFERENCES

1. R. Becker, Z. Physic, 8, 321 (1922); Z. Electrochem 42, 457 (1936).

2. R. Kling and A. Mamam, "Detonation in Shock Wave Ignited Kerosene-Air Mixtures", Eighth Symposium (International) on Combustion, p. 1096, Williams and Wilkins, Baltimore, (1962).

3. F. B. Cramer, "The Onset of Detonation in a Droplet Combustion Field", Ninth Symposium (Int) on Combustion, p. 482, Academic Press, New York (1963).

4. R. P. Frazer, "Detonation Velocities in Liquid Fuel Vapors with Air or Oxygen at 100°C and at Atmospheric Pressure", p. 783, Seventh Symposium (Int) on Combustion, Butterworths Scientific Publications, London (1959).

5. J. A. Nichols, E. K. Dabora and K. W. Ragland, "A Study of Two Phase Detonation as it Relates to Rocket Motor Combustion Instability", NASA CR-242, (August 1965).

6. I. Hartman and H. P. Grenwald, "The Explosibility of Metal-Powder Dust Clouds", Mining and Metallurgy, V. 26, p. 331 (1945).

7. H. M. Cassell, A. K. Das Gupta and S. Guruswamy, "Factors Affecting Flame Propagation Through Dust Clouds", Third Symposium (Int) on Combustion, p. 185, Williams & Wilkins Co. (1949).

8. A. V. Grosse and J. B. Conway, Industrial Engineering and Chemistry, Vol. 50, p. 663, April 1958.

9. R. Edse, N. K. Rao, W. A. Strauss and M. E. Mickelson, Journal of the Optical Society of America, Vol. 53, No. 4, p. 436 (April 1963).

10. B. J. McBride, S. Heimel, J. G. Ehlers, and S. Gorden, "Thermodynamic Properties to 6000°K for 210 Substances Involving the First 18 Elements", National Aeronautics and Space Administration Report NASA SP-3001 (1963).

11. W. H. Jones, T. O. Dobbins and B. K. Farris, "JANAF Thermochemical Data", Thermal Laboratory, The Dow Chemical Company, Midland, Michigan (December 1960).

12. W. A. Strauss and R. Edse, ISA Transactions, Vol. 3, No. 3 (July 1964).

13. J. D. Lyle, Jr., R. J. Towner and J. E. Vruggink, "Aluminum Powders for Solid Propellants", Space and Astronautics, p. 70 (September 1962).

14. I. D. Doig and G. H. Roper, "Energy Requirements in Phenumatic Conveying", Australian Chemical Engineering (February 1963).

15. R. Edse and E. S. Fishburne, Aerothermochemistry, John Wiley and Sons, Inc. (1967), (In print).

16. F. D. Rossini, Chemical Thermodynamics, John Wiley and Sons, Inc. (1950).

17. E. A. Mickle, "Collected Thermodynamic Properties of 88 Possible Products of Reaction", Aircraft Gas Turbine Division, General Electric Company, Report DF 58A6T111 (December 1957).

18. L. Brewer and A. W. Searcy, J. Am. Chem. Soc., 73, p. 5308, (1951).

19. J. Drowart, G. DeMaria, R. Burns and M. G. Inghram, J. Chem. Physics, 32 (5), p. 1366 (1960).

20. B. F. Dodge, Chemical Engineering Thermodynamics, McGraw Hill Book Co., New York and London (1944).

21. A. D. Kirshenbaum and J. A. Cahill, J. Inorganic Nuclear Chem., Vol. 14, p. 283 (1960).

22. F. J. Zeleznik and S. Gorden, "A General IBM 704 or 7090 Computer Program for Computation of Chemical Equilibrium Compositions, Rocket Performance, and Chapman-Jouquet Detonations", NASA Technical Note D-1454 (October 1962).

23. R. F. Hoglund, "Recent Advances in Gas Particle Nozzle Flows," ARS Journal (May 1962).

24. B. Lewis and G. von Elbe, Combustion, Flames and Explosions of Gases, Academic Press Inc., New York (1961).

25. D. H. Edwards, G. T. Williams and J. C. Breeze, J. of Fluid Mechanics, Vol. 6 (4), p. 497 (1959).

26. A. J. Mooradian and W. E. Gordens, J. of Chem. Physics, No. 19, p. 1166 (1951).

27. F. J. Martin, P. H. Kydd and G. W. Browne, "Condensation of Products in Diborane-Air Detonations", Eighth Symposium (Int) on Combustion, p. 633, The Williams and Wilkins Co., Baltimore (1962).

28. S. W. Gouse, Jr. and G. A. Brown, "Some Remarks on the Velocity of Sound for Two Phase Mixtures and Flows", Office of Naval Research Report on Contract Nour-184(52), D.S.R. Proj. 840, (April 1963).

29. E. A. Gulbransen and W. S. Wysong, J. Physical and Colloid Chemistry, V. 51, p. 1087 (1947).

30. F. Keller and J. D. Edwards, "The Behavior of Oxide Films on Aluminum", Pittsburg International Conference on Surface Reaction, Corrision Publishing Co., Pittsburg (1948).

31. F. J. Martin and D. R. White, "The Formation and Structure of Gaseous Detonation Waves", Seventh Symposium (Int) on Combustion, p. 856, Butterworths Scientific Publications, London (1959).

32. W. A. Bone, R. P. Fraser and W. H. Wheeler, Phil. Trans. Roy. Soc. (London), A-235, p. 29 (1936).

33. A. K. Oppenheim, A. J. Laderman and P. A. Urtiew, Combustion and Flame, V. 6, No. 3, p. 193 (1962).

34. J. A. Laughrey, L. E. Bollinger and R. Edse, "High-Speed Photographic Investigation of the Formation of Detonation Waves in a Stoichiometric Hydrogen-Oxygen Mixture", NASA TN D-2242 (1964).

35. L. E. Bollinger, M. C. Fong and R. Edse, "Experimental Measurements and Theoretical Analysis of Detonation Induction Distances", ARS Journal (May 1961).

36. R. A. Dobbins and S. Tempkin, "Measurements of the Attenuation of Sound by Suspended Particles", Div. of Engineering, Brown University, Providence, Rhode Island (March 1964).

37. G. F. Carrier, J. of Fluid Mechanics, V. 4, p. 376 (1958).

38. C. Campbell and A. C. Finch, J. of the Chem. Soc., No. 11, p. 2094 (1928).

39. J. A. Fay, J. of Chemical Physics, V. 20, No. 6, p. 942 (1952).

40. M. Barrere, A. Jaumotte, B. F. Veubeke and J. Van der Kerckhove, Rocket Propulsion, Elsevier Publishing Co., New York (1960).

41. K. Berman and S. H. Cheney, Jr., J. Am. Rocket Soc., V. 223, No. 2, p. 89 (1953).

42. L. E. Bollinger and R. Edse, "Thermodynamic Calculations of Hydrogen-Oxygen Detonation Parameters for Various Initial Pressures", ARS Journal (February 1961).

43. L. E. Bollinger and R. Edse, "Detonation Induction Distances in Hydrogen-Oxygen and Acetylene-Oxygen-Nitrogen Mixtures at Normal and Elevated Pressures and Temperatures", WADC TR 57-414 (June 1957).

44. E. S. Fishburne and S. L. Petrie, "Spectrographic Determination of Temperature and Specie Concentrations of High Temperature Gases", The Ohio State University Research Foundation (February 1963).

45. A. Goldsmith, T. E. Waterman and H. J. Hinschhorn, Handbook of Thermophysical Properties, Vol. I and Vol. III, Pergamon Press, New York, Oxford, London, Paris (1961).

46. C. A. Barth, Annals de Geophysique, Vol. 20, No. 2, p. 182, April-June 1964.

SYMBOLS

a	= activity of species
d	= differential
dia	= combustion tube diameter
f	= frequency
c	= sound speed
c_v	= specific heat at constant volume
(g)	= gaseous species
h	= specific enthalpy
k	= reaction rate coefficient
n	= specific molality (per unit mass of mixture)
n^g	= specific molality (per unit mass of gas mixture)
oxide	= decimal equivalent of mass of alumina oxide to total mass of powder
p	= pressure
t	= time
u	= velocity
u_p	= particle velocity behind detonation wave
u_1	= detonation velocity
v	= specific volume
$\Delta H_f^{i,T}$	= molar heat of formation of species i at temperature T
K	= equilibrium constant in terms of p_i of species

N_i = total number of elements of species i in a given mixture

M = molecular weight

(M_i) = concentration of species i

$\mathcal{R}$ = universal gas constant

T = temperature

$\mathcal{K}$ = ratio of oxygen mass to aluminum powder mass in mixture

$\alpha = N_{Al}/N_o$ = ratio of elemental aluminum particles to oxygen particles

$\overline{\alpha}$ = a constant

γ = ratio of specific heats

ρ = density

λ = wavelength of flame oscillations

Subscripts

1 = initial conditions (unreacted state)

2 = stable detonation conditions (reacted state)

3 = 3-body collision

f = flame

Al = aluminum powder

F = foreward

g = gas

i = species

liq = liquid

m = mixture

ox = oxidizer

R = reverse

AUTOBIOGRAPHY

I, William A. Strauss, was born in Cleveland, Ohio on July 20, 1927. I received my secondary school education in the public schools of Euclid, Ohio. I received a Bachelor of Mechanical Engineering degree from The Ohio State University in 1950. I worked as a Research Associate at The Ohio State University Rocket Research Laboratory and attended Graduate School on a part-time basis during the period of 1951 through 1958. I received a Masters degree from the Aeronautical Engineering Department and was appointed Assistant Supervisor at the Ohio State University Rocket Research Laboratory. Since receiving my B. of M.E. degree, I have authored or co-authored 16 technical articles in the field of combustion and propulsion

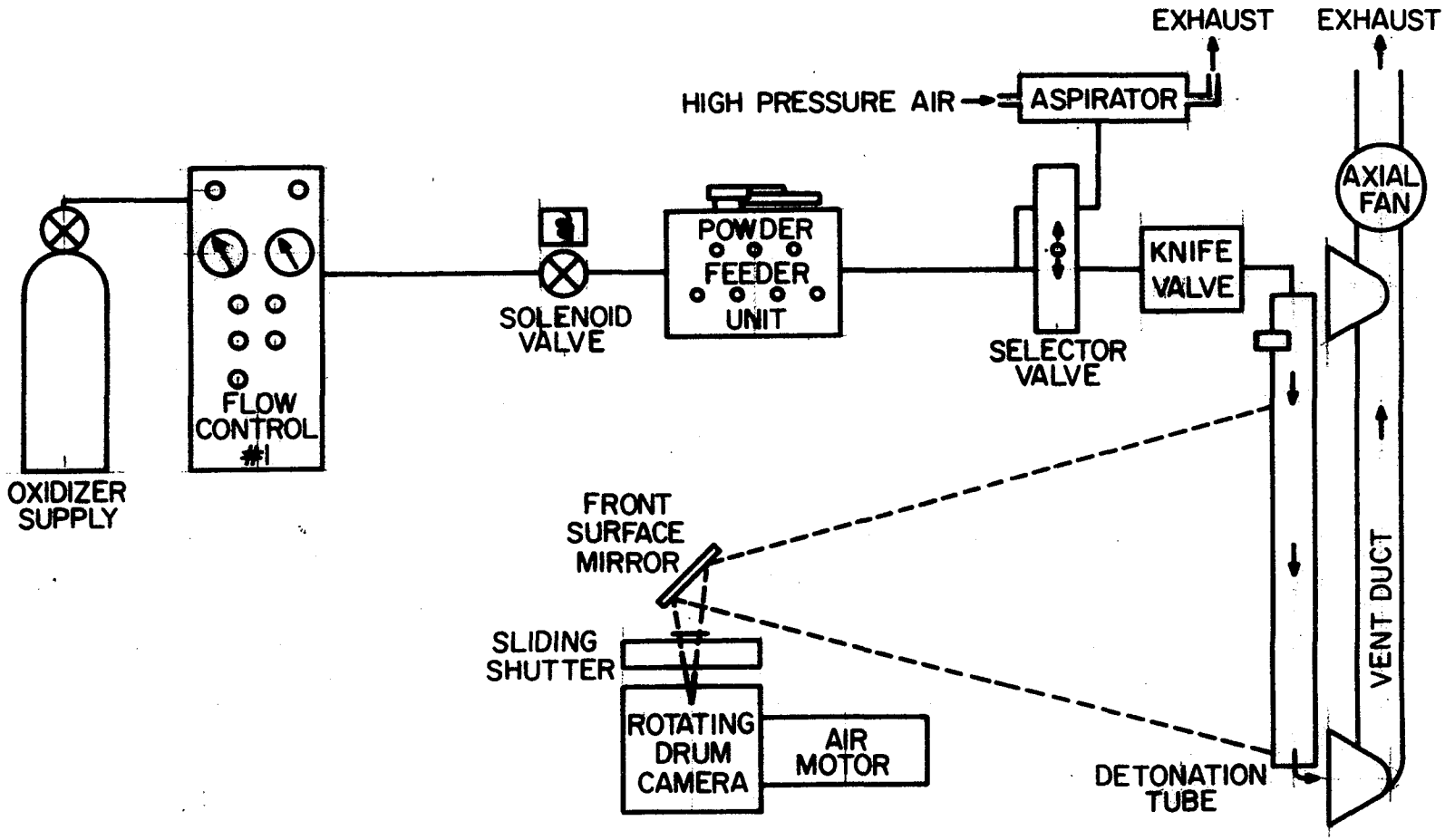

FIGURE 1. HETEROGENOUS DETONATION APPARATUS

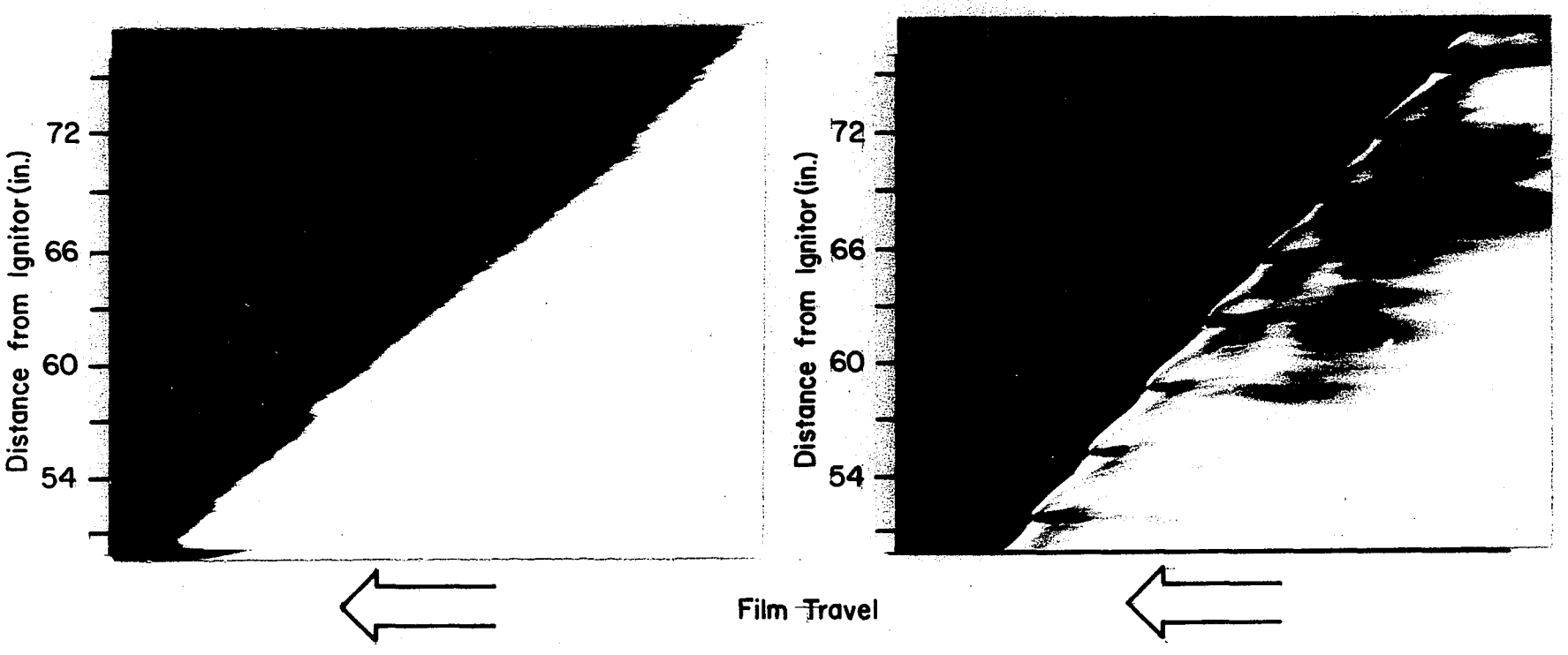

FIGURE 2. TYPICAL STREAK PHOTOGRAPHS OF ALUMINUM POWDER–OXYGEN MIXTURES BURNING IN COMBUSTION TUBES.

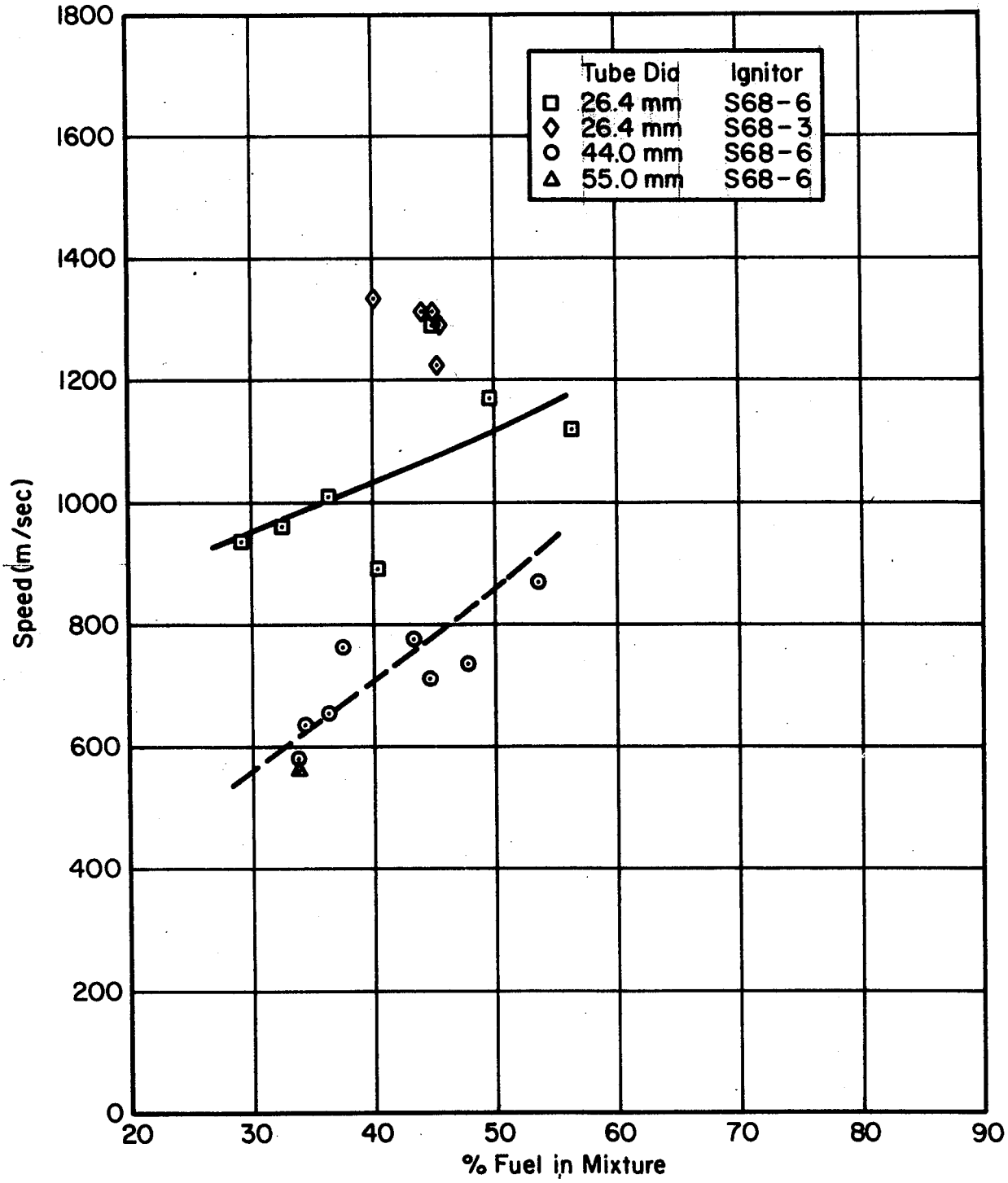

FIGURE 3. FLAME SPEEDS OF SHOCK IGNITED FLAKE ALUMINUM POWDER-OXYGEN MIXTURES.

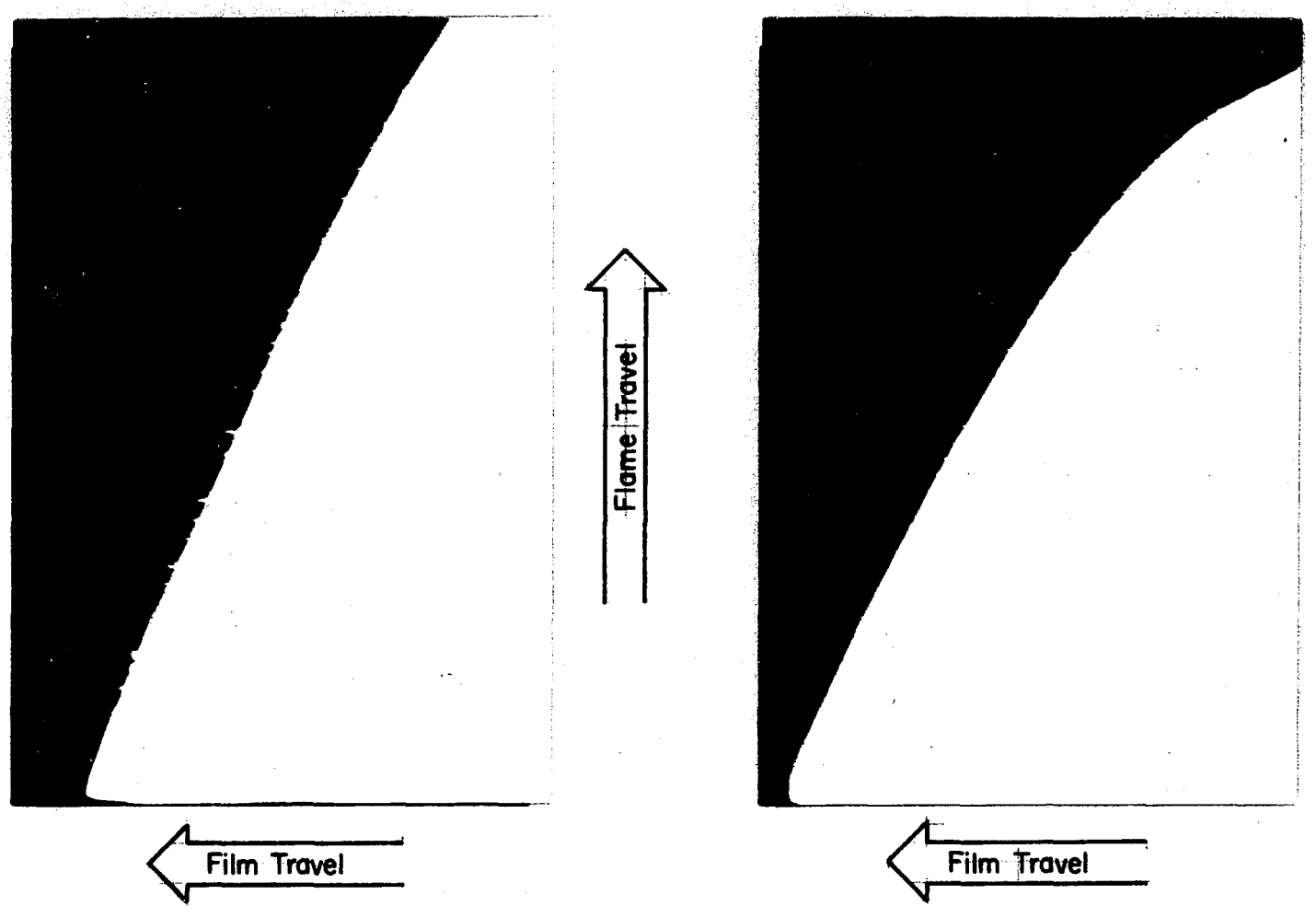

FIGURE 4. DECELERATING FLAMES PROPAGATING IN LEAN ALUMINUM POWDER–OXYGEN MIXTURES.

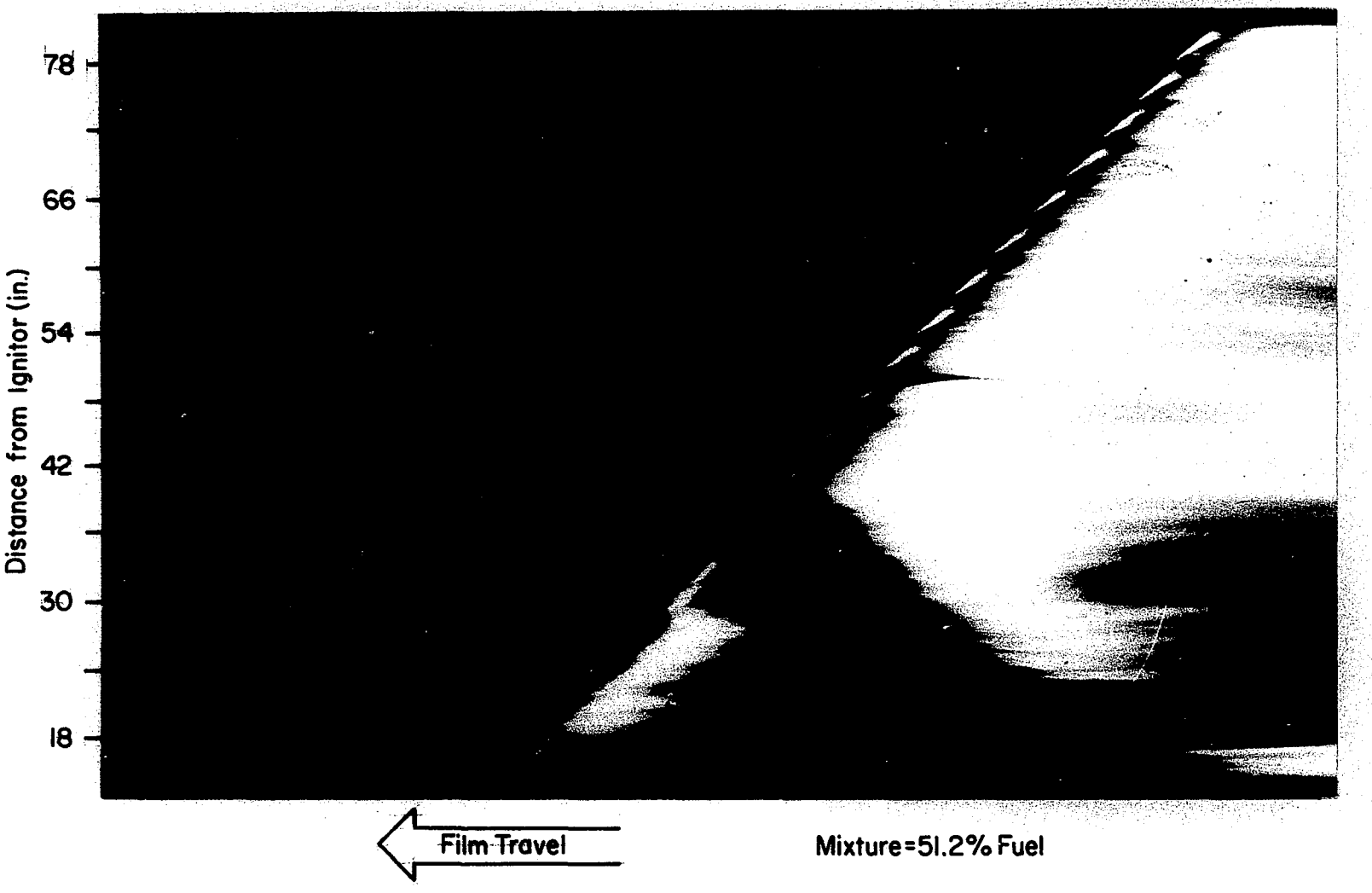

FIGURE 5. TYPICAL STREAK PHOTOGRAPH OF A RICH ALUMINUM POWDER–OXYGEN MIXTURE FLAME.

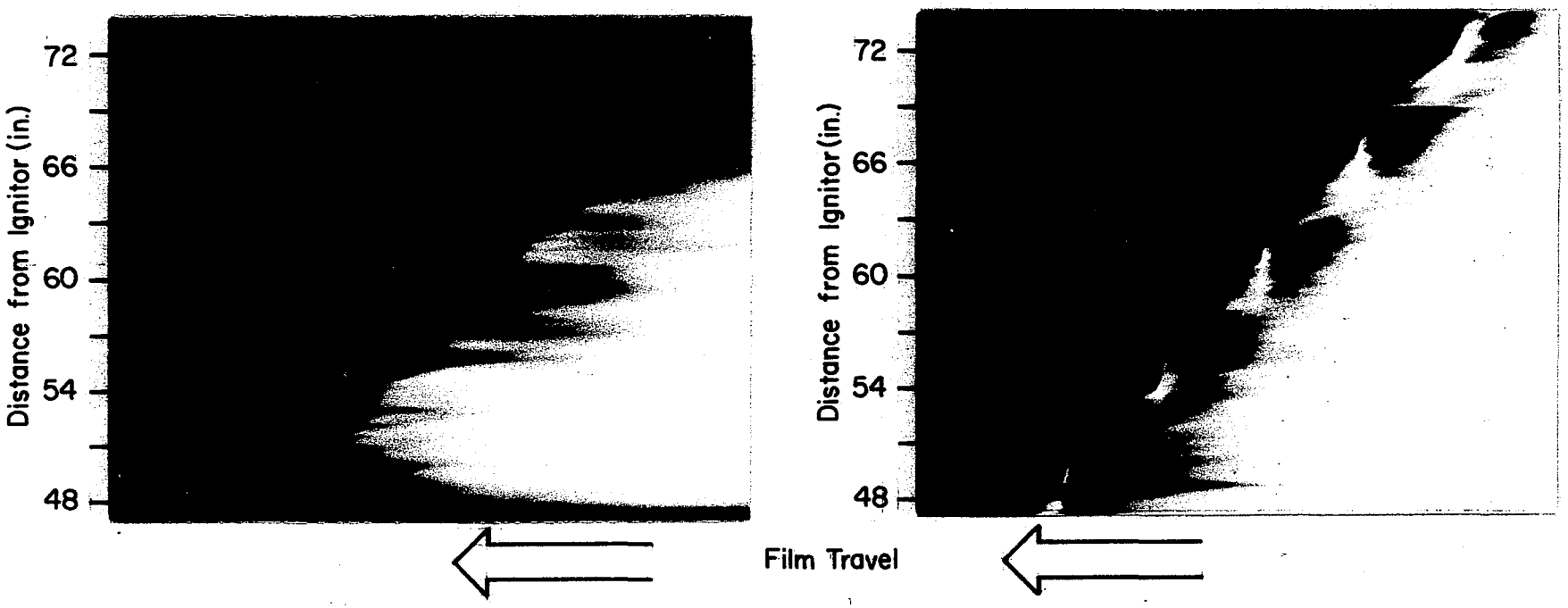

FIGURE 6. PHOTOGRAPHS OF DETONATING FLAKE ALUMINUM POWDER-OXYGEN MIXTURES IN VARIOUS DIAMETER TUBES.

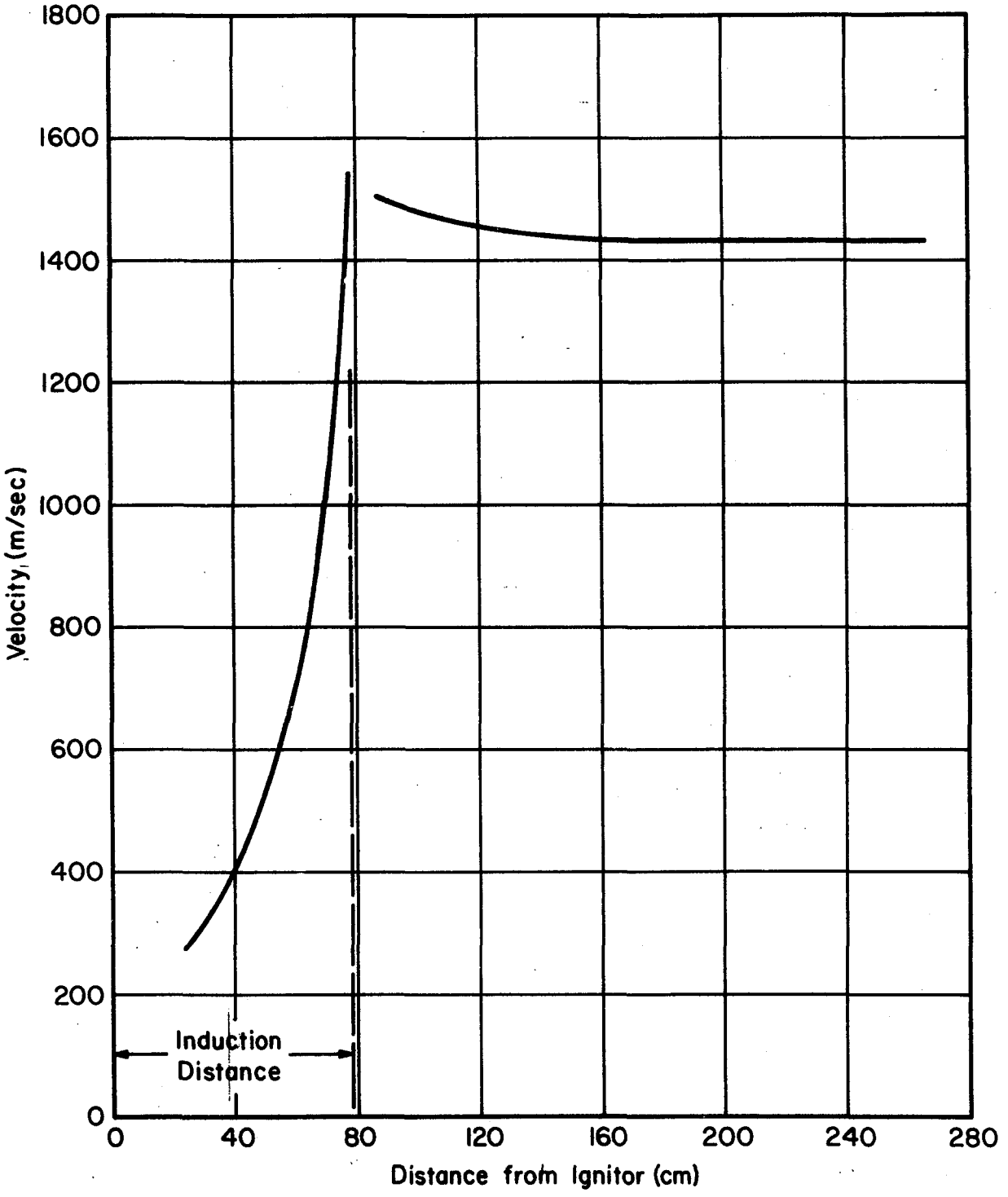

FIGURE 7. PLOT OF FLAME VELOCITY AS A FUNCTION OF DISTANCE FROM POINT OF IGNITION.

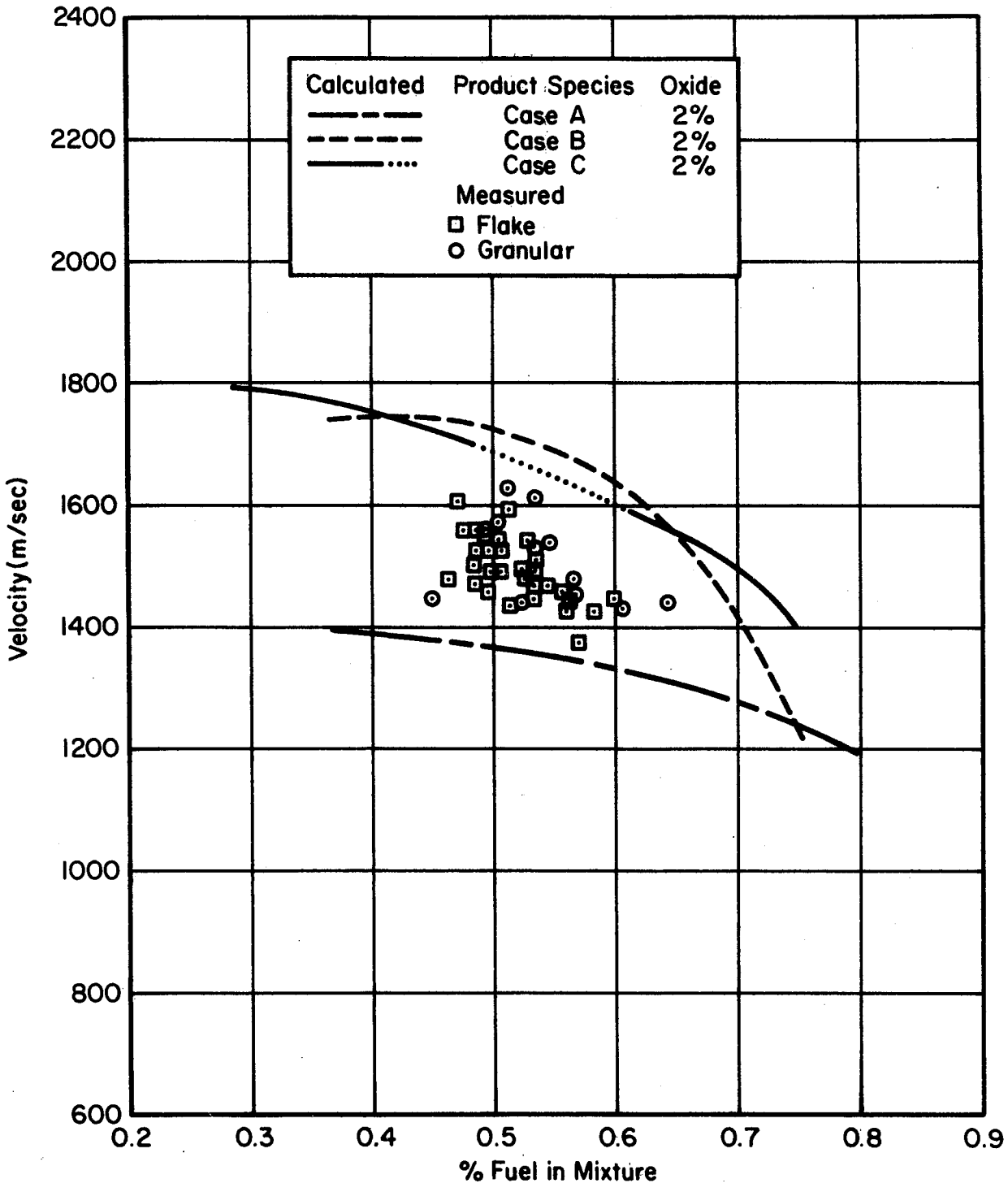

FIGURE 8. DETONATION VELOCITIES OF ALUMINUM POWDER-OXYGEN MIXTURES.

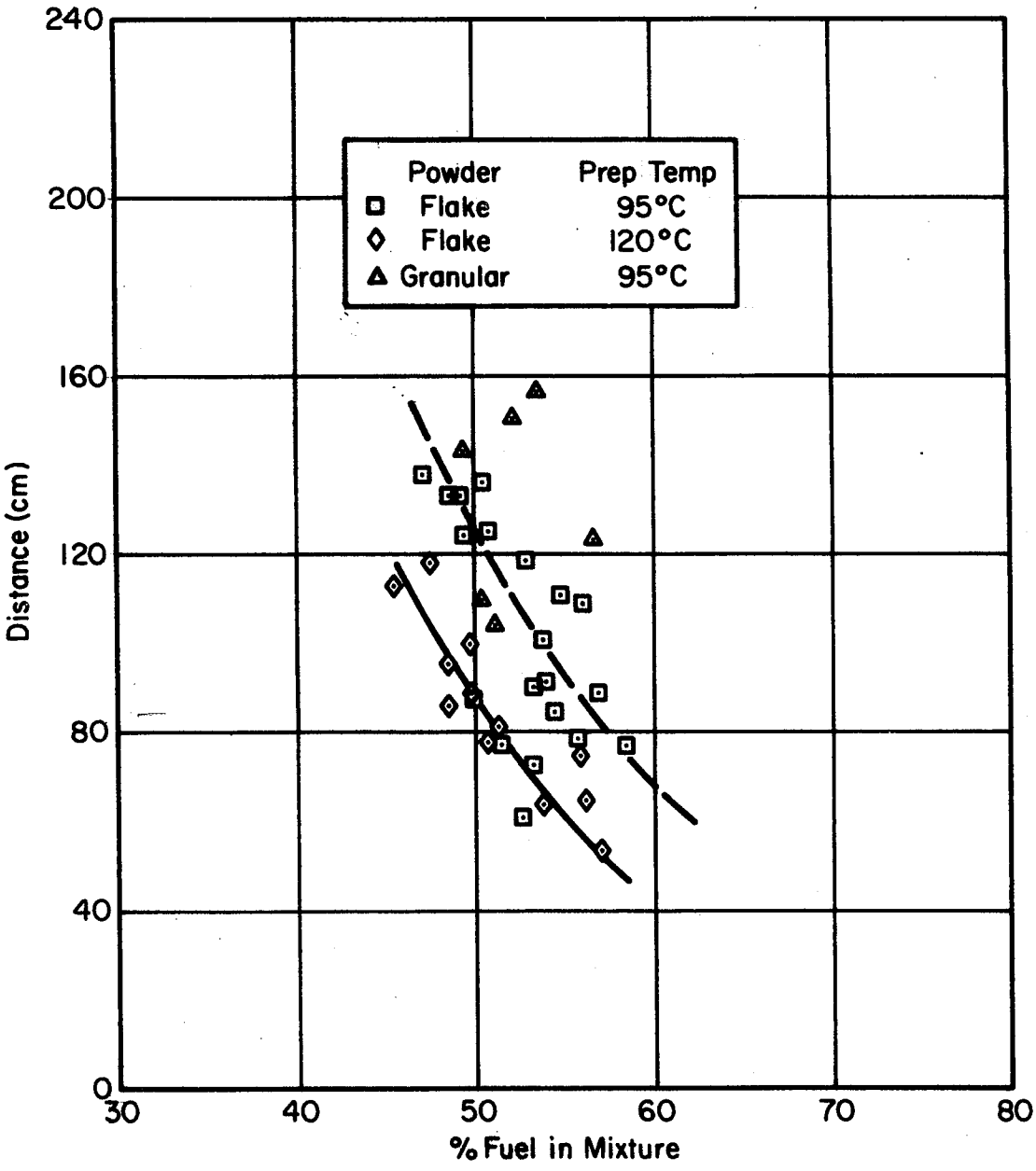

FIGURE 9. DETONATION INDUCTION DISTANCES OF ALUMINUM POWDER-OXYGEN MIXTURES.

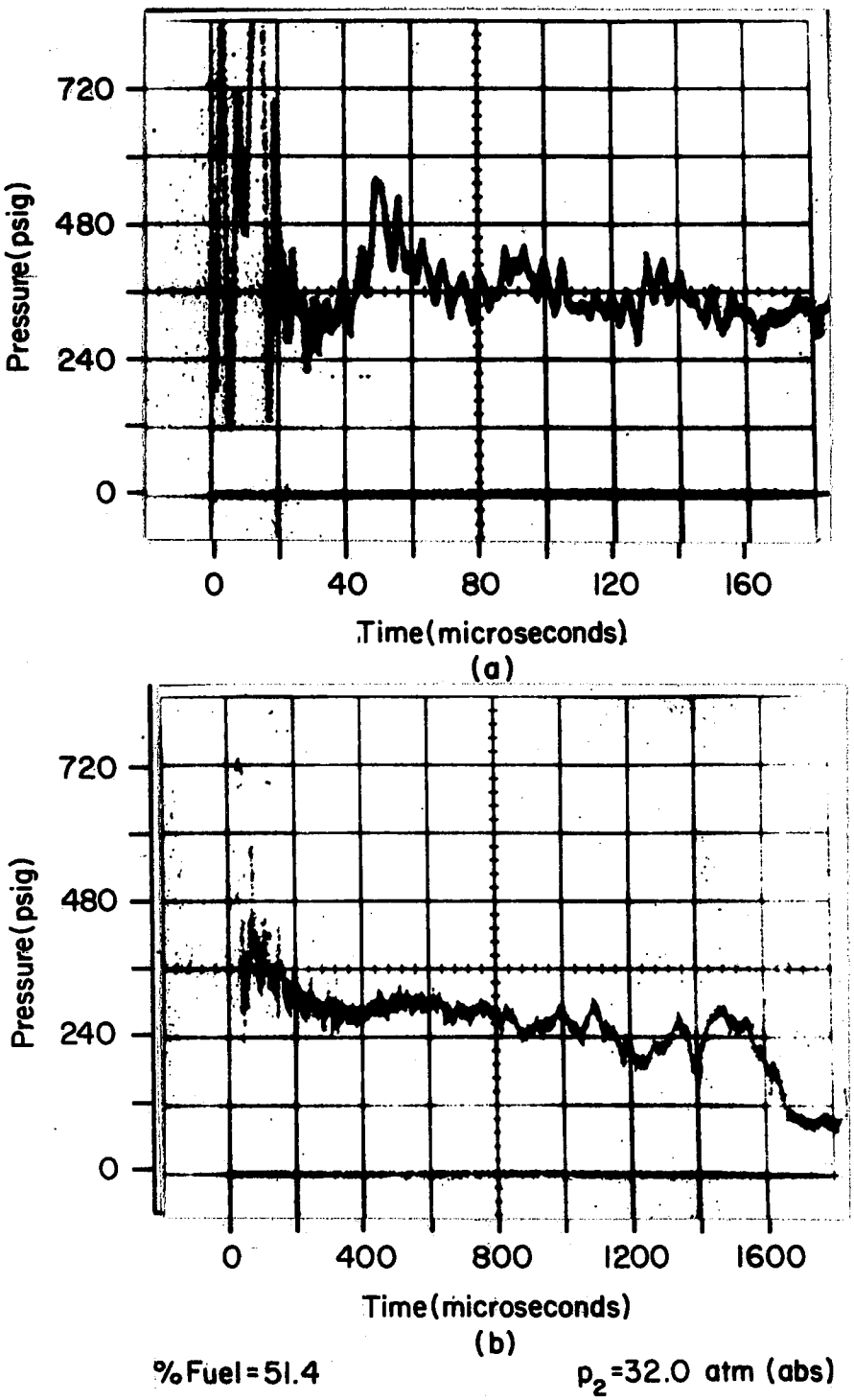

FIGURE 10. TYPICAL PLOTS OF PRESSURE VERSUS TIME FOR A DETONATING FLAKE ALUMINUM POWDER-OXYGEN MIXTURE.

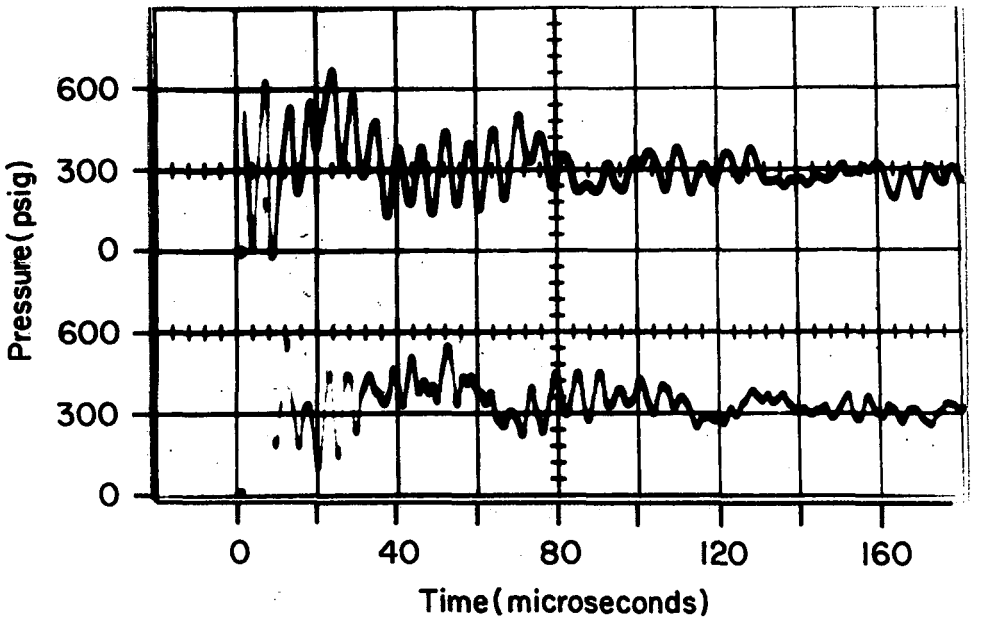

FIGURE 11. TYPICAL PLOTS OF PRESSURE VERSUS TIME FOR A DETONATING ALUMINUM POWDER-OXYGEN MIXTURE (FROM OPPOSED PRESSURE TRANSDUCERS).

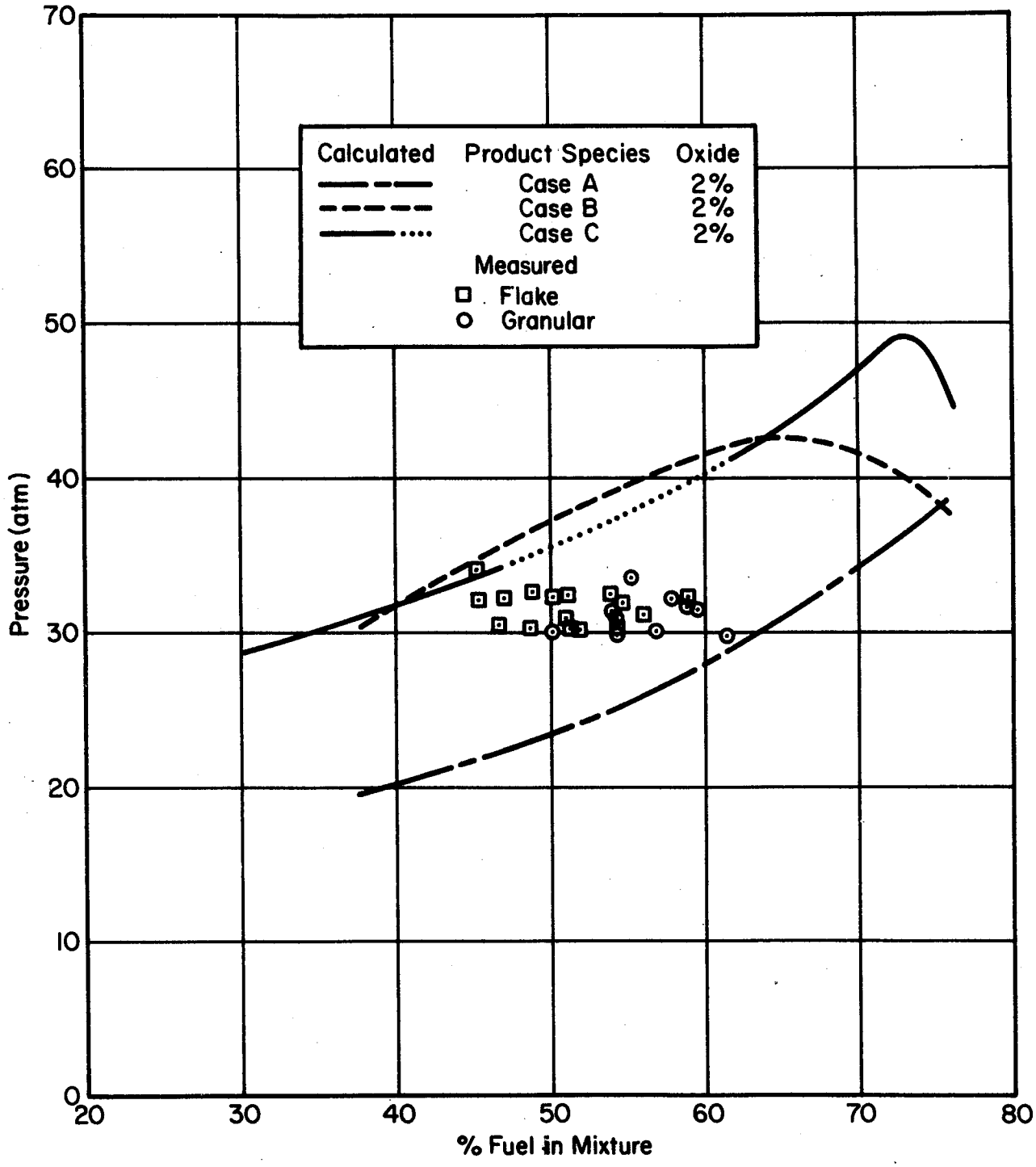

FIGURE 12. DETONATION PRESSURES OF ALUMINUM POWDER-OXYGEN MIXTURES.

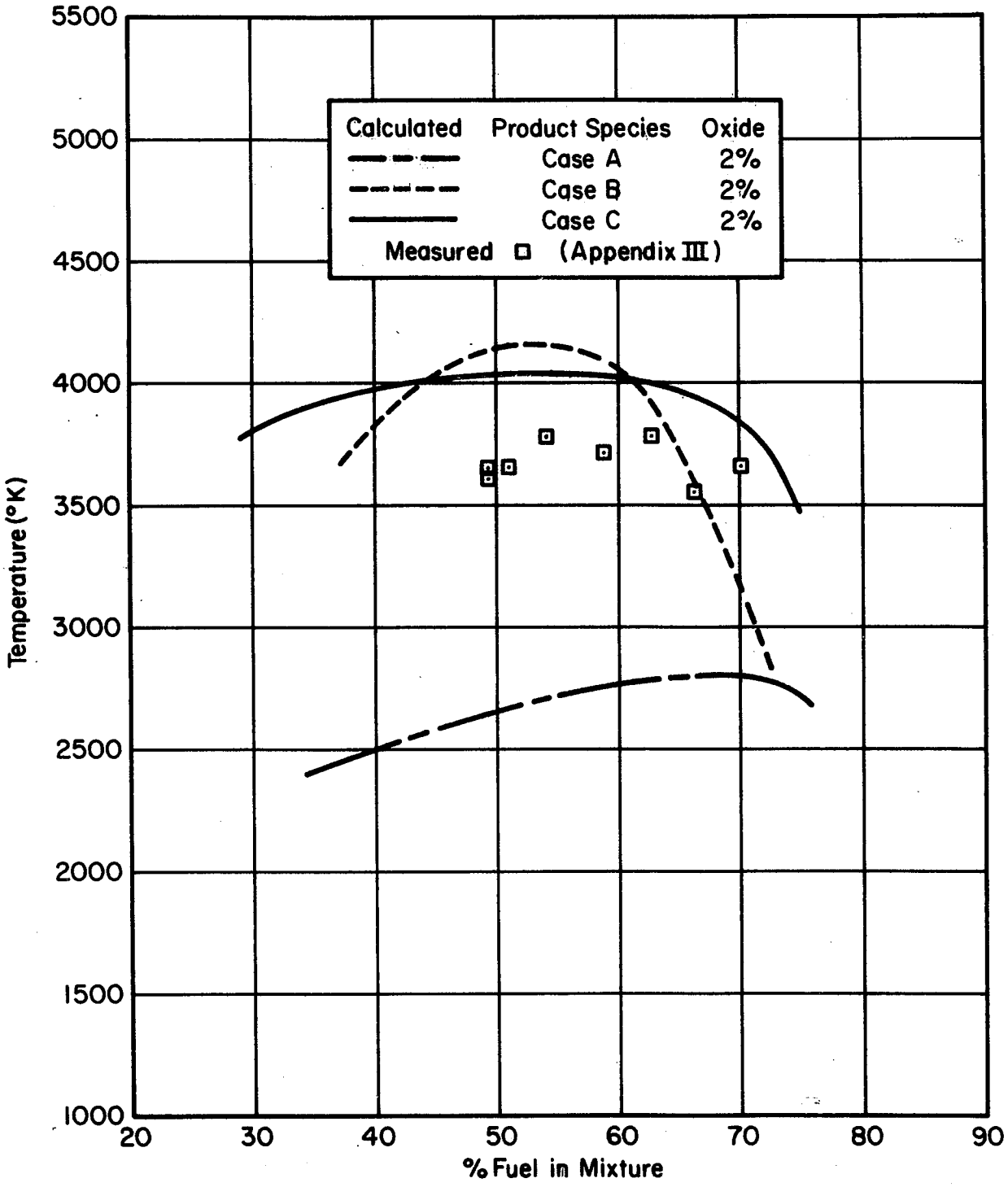

FIGURE 13. ADIABATIC FLAME TEMPERATURES OF ALUMINUM POWDER-OXYGEN MIXTURES.

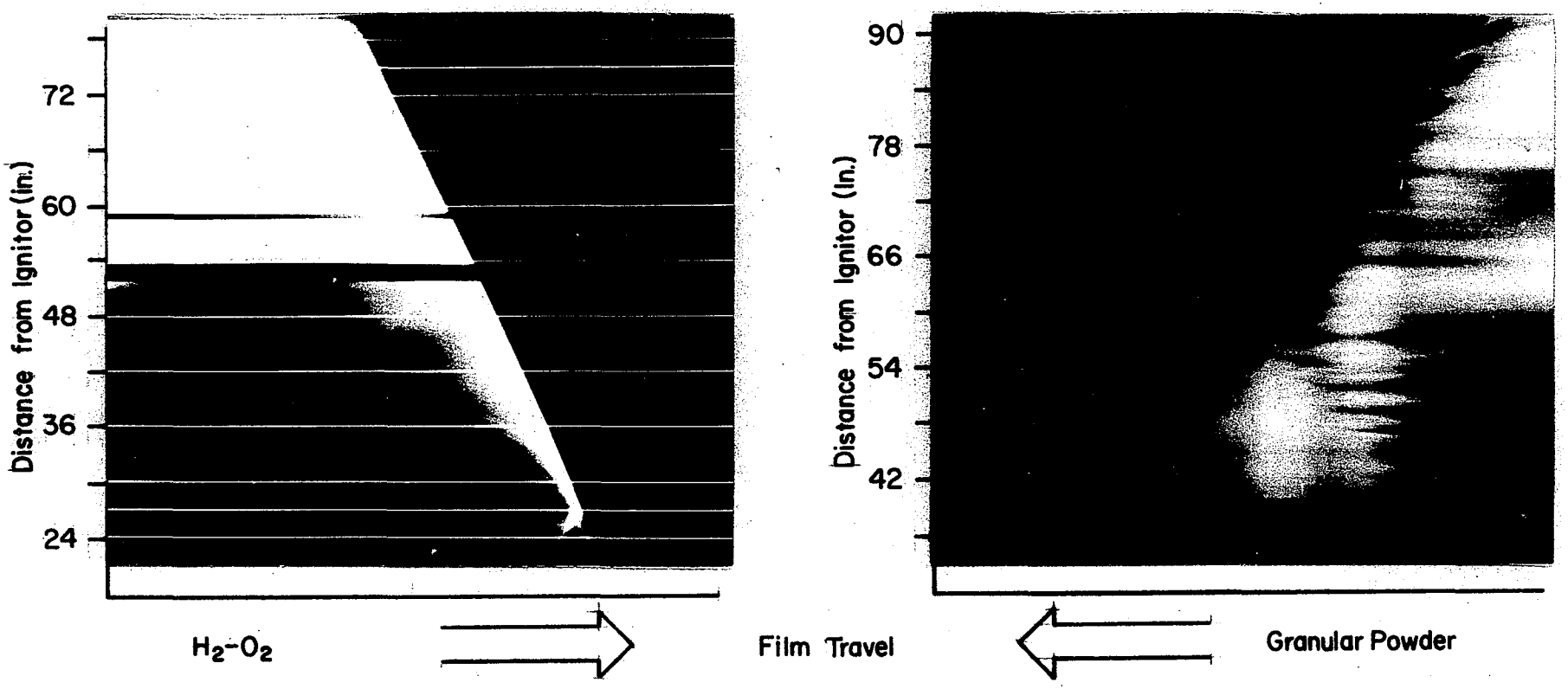

% H_2 In Mixture = 68.1
u_1 = 2893 m/sec

(a)

% Al In Mixture = 49.3
u_1 = 1560 m/sec

(b)

FIGURE 14. STREAK PHOTOGRAPHS OF A DETONATING HYDROGEN-OXYGEN MIXTURE AND A DETONATING ALUMINUM POWDER-OXYGEN MIXTURE.

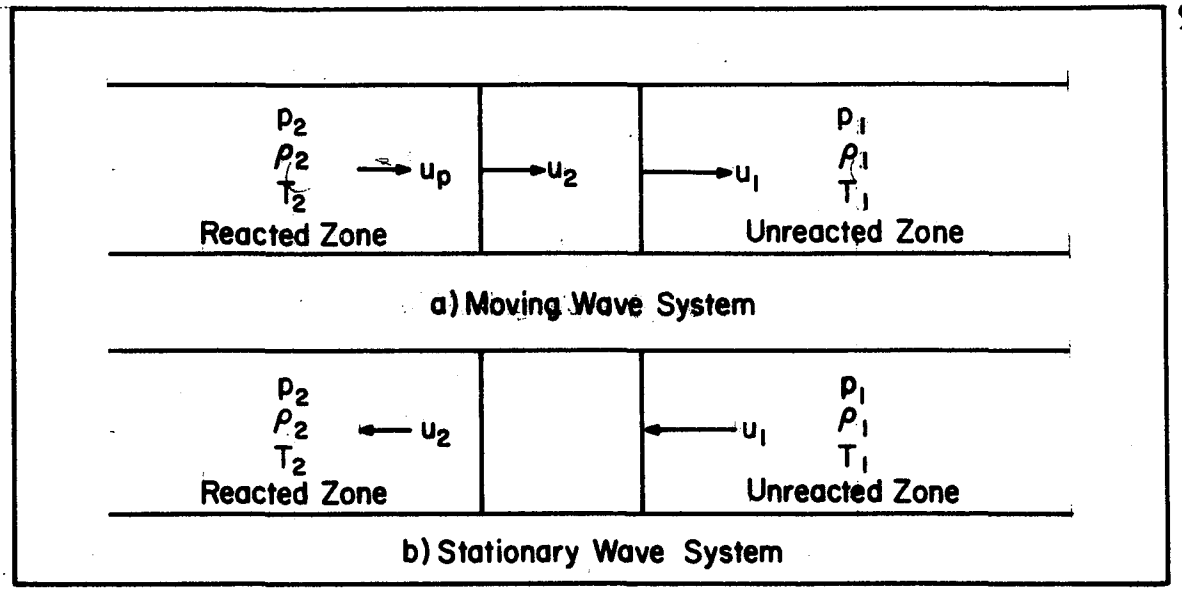

FIGURE 15. SYSTEMS OF FLOW THROUGH A DETONATION WAVE.

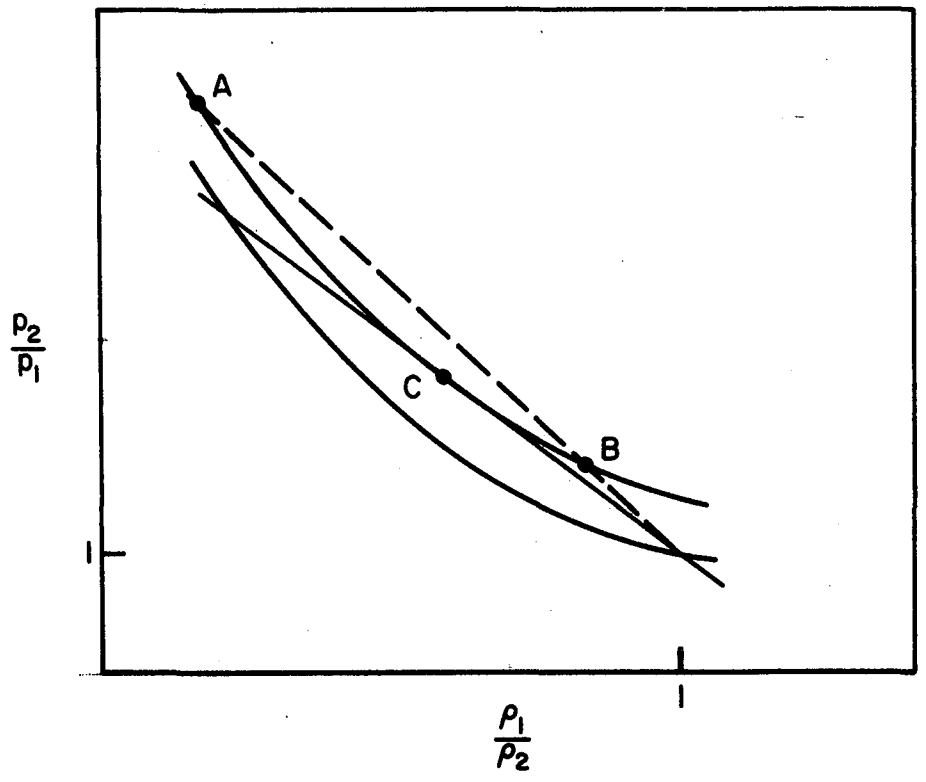

FIGURE 16. RALEIGH LINES AND HUGONIOT CURVES.

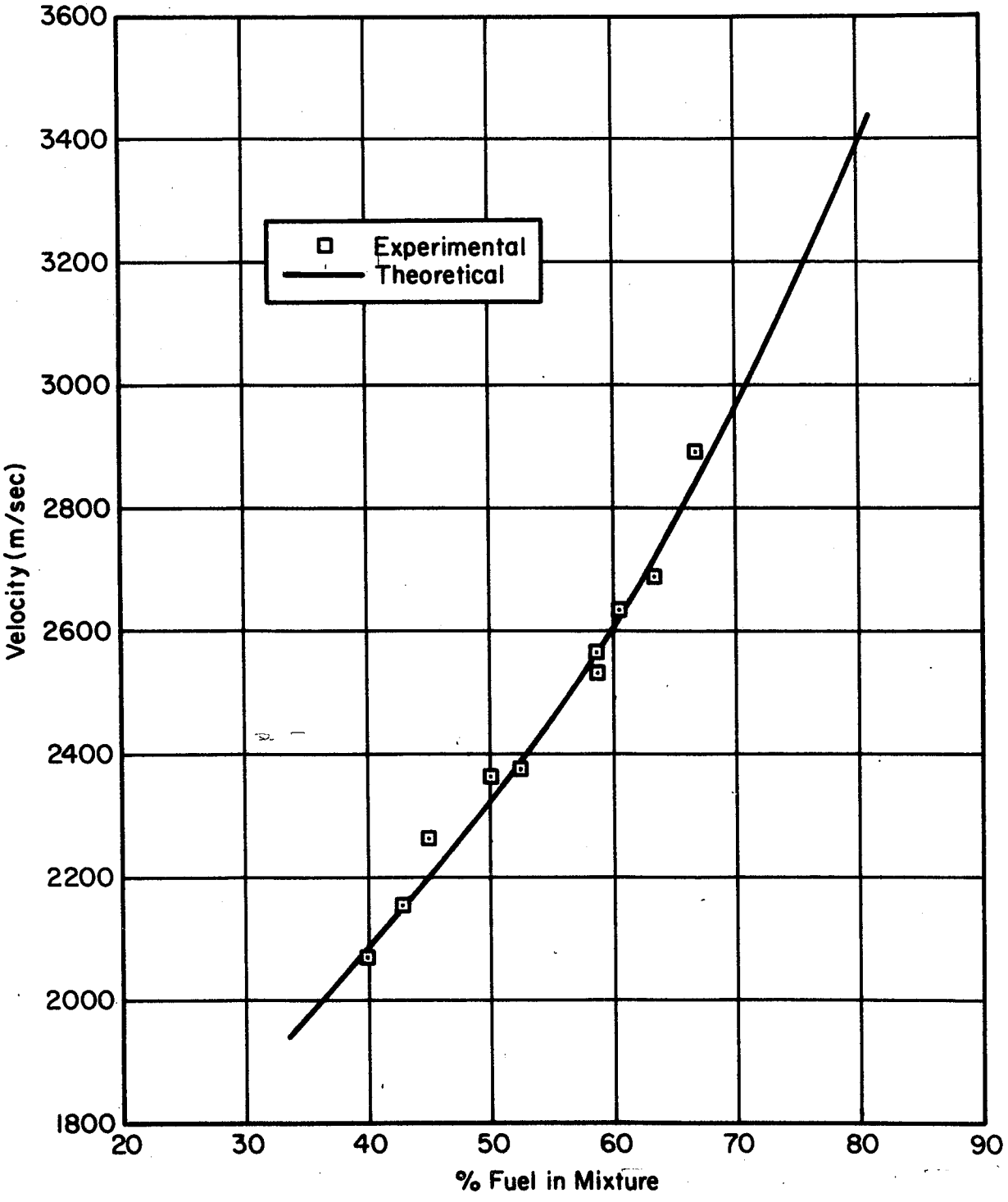

FIGURE 17. DETONATION VELOCITIES OF HYDROGEN-OXYGEN MIXTURES.

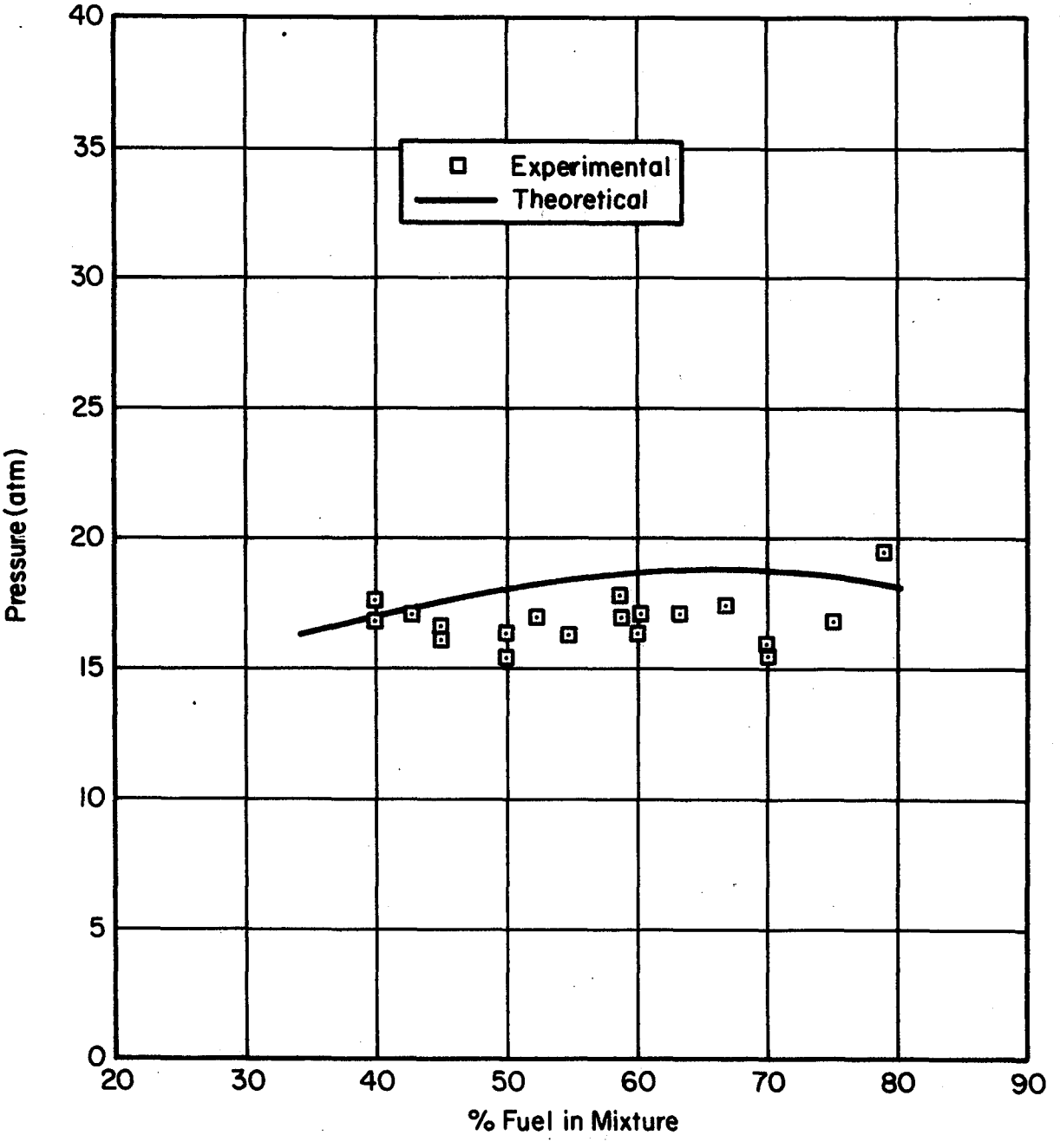

FIGURE 18. DETONATION PRESSURES OF HYDROGEN-OXYGEN MIXTURES.

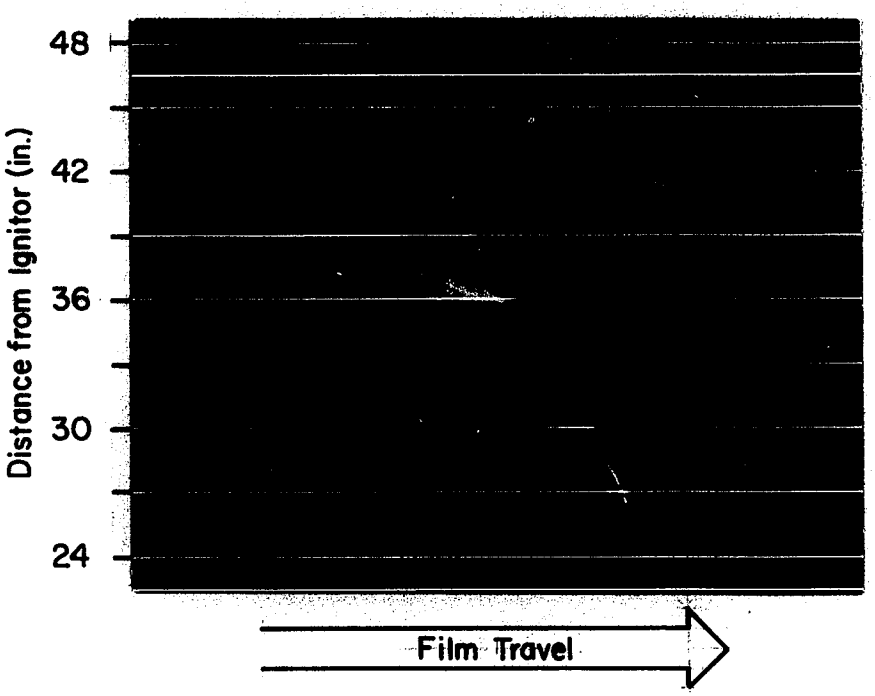

% Hydrogen in Mixture = 44.6
u_1 = 2224 m/sec
dia = 26.4 mm

FIGURE 19. TYPICAL STREAK PHOTOGRAPH OF A DETONATING HYDROGEN-OXYGEN MIXTURE.

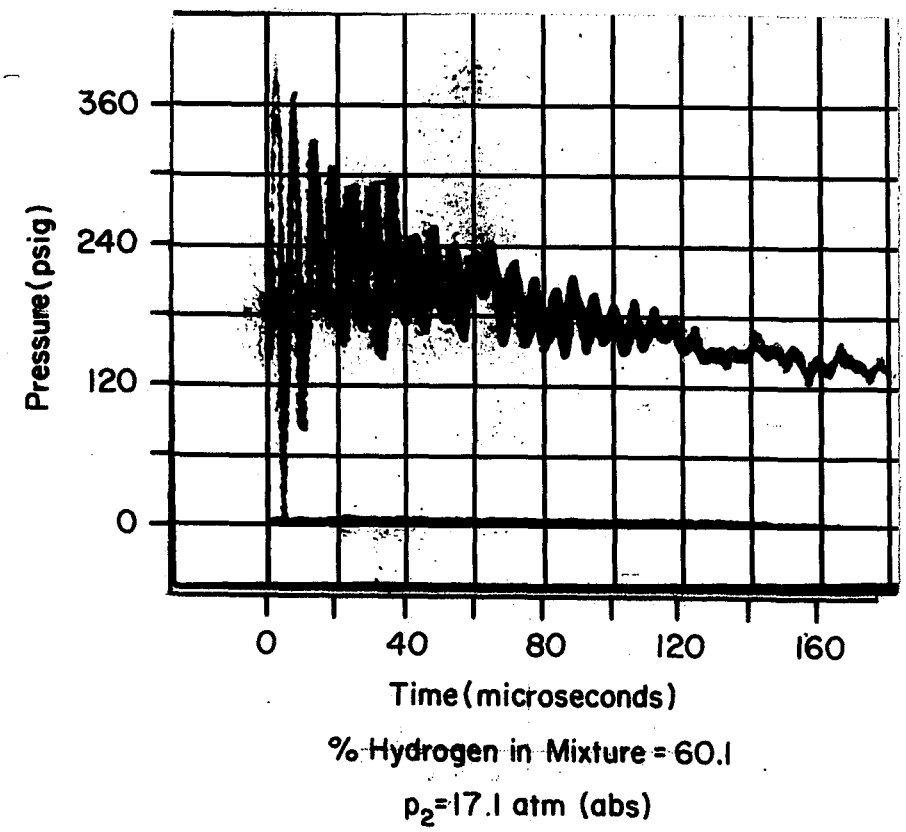

FIGURE 20. TYPICAL PLOT OF PRESSURE VERSUS TIME FOR A DETONATING HYDROGEN-OXYGEN MIXTURE.

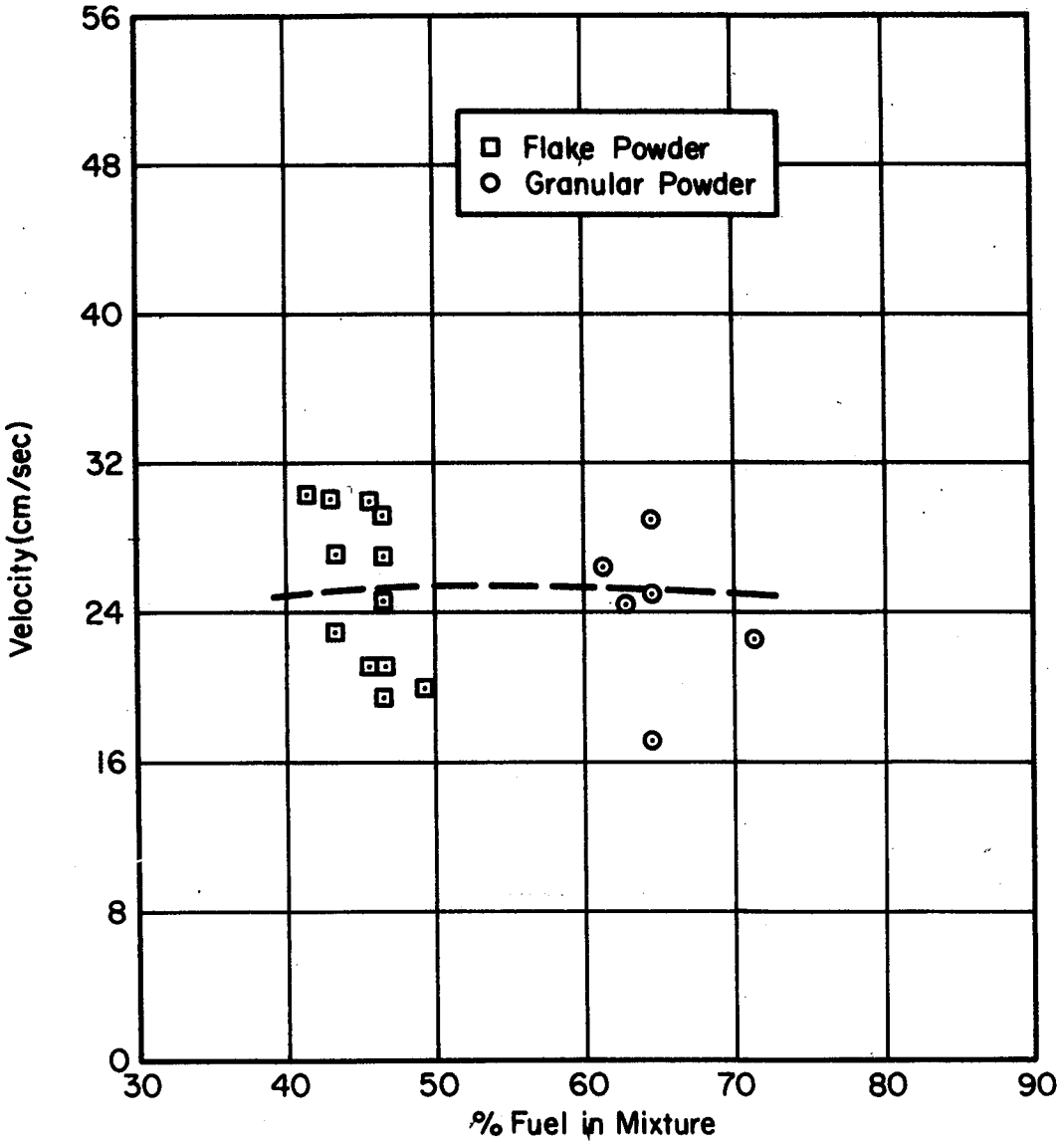

FIGURE 21. BUNSEN-BURNER FLAME VELOCITIES OF ALUMINUM POWDER-OXYGEN MIXTURES.

TABLE 1. Measured Flame Speeds of Shock Ignited Aluminum Powder-Oxygen Mixtures

Initial Conditions: Room Temperature
Atmospheric Pressure

Tube Dia. = 26.4mm			Tube Dia. = 44.0mm			Tube Dia. = 55.2mm		
% Fuel	u_f (m/sec)	Ignitor	% Fuel	u_f (m/sec)	Ignitor	% Fuel	u_f (m/sec)	Ignitor
29.2	935	S68-6	33.9	576	S68-6	-	-	-
32.6	960	S68-6	34.2	636	S68-6	-	-	-
36.4	1010	S68-6	36.2	654	S68-6	-	-	-
40.1	1333	S68-3	37.3	763	S68-6	38.3	566	S68-6
40.2	891	S68-6	-	-	-	-	-	-
44.1	1311	S68-3	43.1	676	S68-6	-	-	-
44.9	1310	S68-3	44.5	711	S68-6	-	-	-
45.0	1290	S68-6	-	-	-	-	-	-
45.2	1290	S68-3	-	-	-	-	-	-
45.4	1225	S68-3	-	-	-	-	-	-
47.6	1370	FP	47.8	718	S68-6	-	-	-
49.8	1170	S68-6	-	-	-	-	-	-
51.1	1140	FP	53.4	870	S68-6	-	-	-
56.4	1120	S68-6	-	-	-	-	-	-

FP Flash Powder Squib
S68-3 Generating Squib (3 Grain)

TABLE 2. Measured Detonation Parameters of Flake Aluminum Powder-Oxygen Mixtures

Initial Conditions: Room Temperature
Atmospheric Pressure
Exploding Silver Wire Ignitor (+ Pressure Generating Squib)

% Fuel	Tube Dia. (mm)	Induction Distance (cm)	u_1 (m/sec)	Flame Spin λ (cm)	Flame Spin f (1/sec)	Flame Spin λ/dia.
46.1	26.4	113*	1480	9.14	16170	3.46
47.0+	26.4	138	1606	9.14	17560	3.46
47.5	26.4	118*	1559	9.04	17230	3.42
48.4	26.4	95*	1500	9.65	16590	3.66
48.5	26.4	86*	1560	8.99	17340	3.41
48.5+	26.4	85	1470	8.79	16720	3.33
48.7	26.4	133	1524	9.58	15910	3.63
49.1	26.4	133	1552	8.94	17360	3.39
49.3	26.4	124	1550	9.35	16580	3.54
49.6	26.4	100*	1457	10.20	14270	3.87
49.7	26.4	89*	1522	10.26	15120	3.89
49.9	26.4	78	1489	9.07	16420	3.43
50.4	26.4	136	1541	9.50	16050	3.60
50.6	26.4	78*	1488	9.12	16310	3.45
50.8	26.4	125	1523	9.53	15980	3.61
51.2	26.4	81*	1589	9.07	17510	3.43
51.2	26.4	78	1436	9.17	15650	3.47
52.2	44.0	-	1496	15.49	9640	3.52
52.6	26.4	61	1480	8.84	16740	3.35
52.9	26.4	119	1540	9.07	16960	3.43
53.2	26.4	73	1444	9.32	15490	3.53
53.3	26.4	90	1487	9.07	16400	3.43
53.6	26.4	62*	1468	9.04	16220	3.42
53.8	26.4	101	1506	9.40	16040	3.56
53.8	26.4	91	1445	8.76	16490	3.32
54.3	26.4	85	1468	9.19	15970	3.48
54.5	44.0	-	1464	15.01	9740	3.41
54.8	26.4	111	1472	8.89	16550	3.36
55.6	26.4	78	1457	9.07	16060	3.43
55.8	26.4	75*	1453	9.09	15970	3.44
56.0	26.4	109	1423	8.94	15920	3.38
56.1	26.4	65*	1443	8.99	16050	3.40
56.9	26.4	89	1440	8.99	16010	3.40
57.0	26.4	54*	1374	9.04	15190	3.42
58.3	26.4	77	1426	8.86	16080	3.35
60.0	26.4	-	1445	-	-	-

*Powder prepared in oven at 120°C. All other experiments had Powder prepared at 95°C.

TABLE 3. Measured Detonation Parameters of Granular Aluminum Powder-Oxygen Mixtures

Initial Conditions: Room Temperature
Atmospheric Pressure
Exploding Silver Wire Ignitor

% Fuel	Tube Dia. (mm)	Induction Distance (cm)	u_1 (m/sec)	Flame Spin λ (cm)	Flame Spin f (1/sec)	Flame Spin λ/dia.
45.0	26.4	-	1436	11.05	12960	4.18
49.3	26.4	143	1560	10.72	14550	4.06
50.3	26.4	110	1571	10.59	14830	4.01
50.7	26.4	-	1558	11.07	14060	4.19
51.1	26.4	104	1627	11.38	14300	4.31
52.3	26.4	151	1440	10.24	14060	3.88
53.1	26.4	-	1521	11.00	13830	4.17
53.5	26.4	156	1610	10.90	14770	4.13
54.6	26.4	-	1539	10.67	14420	4.04
56.3	26.4	-	1449	10.92	13260	4.14
56.6	26.4	123	1579	10.82	14570	4.10
60.2	26.4	-	1533	10.31	14870	3.90
60.2	26.4	-	1525	10.49	14500	3.98
64.1	26.4	-	1540	10.62	14500	4.02

TABLE 4. Measured Detonation Pressures of Aluminum Powder-Oxygen Mixtures

Initial Conditions: Atmospheric Pressure
Room Temperature

Flake Powder		Granular Powder	
% Fuel	p_2(atm)	% Fuel	p_2(atm)
45.3	34.0	50.1	30.0
45.4	32.0	51.6	30.1
46.6	30.5	53.9	31.3
47.0	32.3	54.1	29.8
48.6	30.3	54.3	30.6
48.9	32.6	55.2	33.6
50.8	32.2	56.8	30.1
51.0	30.8	57.7	32.2
51.2	32.4	58.9	31.8
51.3	30.2	59.4	31.5
51.4	32.0	61.3	29.7
52.4	30.0		
53.8	32.5		
54.4	30.2		
54.6	31.9		
56.5	31.1		
58.9	32.2		

TABLE 5. Theoretical Flame Temperatures of Aluminum Powder-Oxygen Mixtures (Case A)

p_1 = 1 atm
T_1 = 298.16°K
Powder oxide content = 2%

% Fuel	T_2 °K	Mole Fractions After Combustion						
		O(g)	O_2(g)	Al(g)	Al_2(g)	AlO(g)	Al_2O(g)	Al_2O_2(g)
37.5	2462.5	.009608	.649327	.000077	-	.012592	.065731	.262665
40.7	2525.0	.012627	.603756	.000152	-	.017940	.094985	.270540
43.6	2575.0	.015408	.559630	.000258	-	.023440	.126315	.274949
48.6	2643.8	.019475	.479754	.000529	-	.033207	.187664	.279371
52.8	2693.8	.022316	.408563	.000887	-	.041906	.249069	.277259
58.0	2743.8	.024163	.315600	.001522	-	.051884	.337311	.269521
63.4	2781.3	.023124	.213449	.002445	-	.059417	.447627	.253938
67.6	2800.0	.019631	.132596	.003434	-	.061327	.552945	.230068
72.4	2790.6	.011117	.045787	.004783	-	.051984	.707124	.179205
75.9	2675.0	.001808	.003147	.004958	-	.022170	.875452	.092466

TABLE 6. Theoretical Flame Temperatures of Aluminum Powder-Oxygen Mixtures (Case B)

p_1 = 1 atm
T_1 = 298.16°K
Powder Oxide Content = 2%

% Fuel	T_2 °K	Mole Fractions After Combustion							
		O(g)	O_2(g)	Al(g)	Al_2(g)	AlO(g)	Al_2O(g)	Al_2O_2(g)	Al_2O_3(g)
37.5	3696.9	.399932	.230364	.001536	-	.003053	.000039	.000002	.335075
40.7	3865.6	.452703	.160644	.007266	-	.008014	.000218	.000005	.371151
43.6	4003.1	.462532	.096745	.025727	-	.016949	.000901	.000013	.397132
48.6	4123.4	.395276	.044992	.096268	.000002	.034882	.004266	.000035	.424278
52.8	4149.2	.304854	.024378	.179057	.000006	.045679	.009397	.000054	.436574
58.0	4109.4	.174736	.009256	.298395	.000018	.050256	.020138	.000076	.447124
63.4	3906.3	.040494	.001088	.433252	.000050	.036334	.049176	.000093	.439513
67.6	3375.0	.000974	.000005	.450525	.000121	.008416	.173670	.000073	.366395
72.4	2831.3	.000004	-	.295147	.000161	.000818	.487857	.000031	.215881

TABLE 7. Theoretical Flame Temperature of Aluminum Powder-Oxygen Mixtures (Case C)

p_1 = 1 atm
T_1 = 298.16°K
Powder oxide content = 2%
*NASA calculations,[22] Powder oxide content = 0.0%

% Fuel	T_2 °K	Mole Fractions After Combustion							
		O(g)	O_2(g)	Al(g)	Al_2(g)	AlO(g)	Al_2O(g)	Al_2O_2(g)	Al_2O_3(liq)
30.0	3802.2	.482114	.293614	.011591	-	.021798	.001554	.000066	.189263
33.9	3887.3	.500957	.225211	.028354	-	.039707	.004785	.000151	.200836
37.5	3937.0	.494767	.181291	.049289	.000001	.056532	.009621	.000248	.208251
40.7	3968.6	.477533	.149912	.072409	.000002	.071368	.015687	.000348	.212742
46.2	4002.5	.429390	.107133	.119768	.000004	.094114	.029935	.000529	.219127
48.6	4010.6	.403065	.091527	.143453	.000006	.102671	.037832	.000609	.220837
57.4*	4011*	.27667*	.04293*	.25475*	.00002*	.12468*	.08123*	.00089*	.21883*
63.9	3997.9	.196190	.000012	.334766	.000035	.124016	.113968	.000950	.230064
65.6	3974.8	.157538	.000007	.364865	.000042	.118208	.130127	.000948	.228265
67.6	3938.7	.114605	.000004	.399679	.000053	.107866	.151122	.000917	.225753
70.9	3829.7	.022326	-	.480717	.000098	.055967	.227299	.000594	.212998
73.7	3600.0	.006765	-	.492452	.000125	.032193	.265161	.000389	.202914
77.0	2575.0	.022326	-	.480717	.000098	.055967	.227299	.000594	.212998

TABLE 8. Theoretical Detonation Properties of Aluminum Powder-Oxygen Mixtures (Case A)

p_1 = 1 atm
T_1 = 298.16°K
Powder Oxide Content = 2%

% Fuel	$\rho_1 \times 10^3$ (gm/cc)	u_1 (m/sec)	p_2 (atm)	T_2 °K	$\rho_2 \times 10^3$ (gm/cc)
37.5	2.09149	1393.7	19.5603	2919.5	3.89396
40.7	2.20412	1389.7	20.3226	2985.9	4.08143
43.6	2.31692	1384.1	21.3723	3043.8	4.33093
48.6	2.54304	1371.1	22.8127	3127.7	4.72967
52.8	2.76986	1357.4	24.5346	3193.8	5.19913
58.0	3.11139	1338.0	26.7792	3265.0	5.85890
63.4	3.56924	1314.6	29.5896	3328.1	6.72961
67.6	4.02992	1294.0	32.2589	3364.5	7.59506
72.4	4.72632	1265.4	36.1042	3368.8	8.91809
75.9	5.42925	1229.4	38.6137	3246.9	10.13715

TABLE 8 (Contd.)

% Fuel	Mole Fractions After Combustion						
	O(g)	O_2(g)	Al(g)	Al_2(g)	AlO(g)	Al_2O(g)	Al_2O_2(g)
37.5	.015374	.645217	.000199	-	.022626	.087368	.229216
40.7	.018395	.599588	.000326	-	.029158	.115418	.237117
43.6	.021027	.556312	.000484	-	.035582	.144288	.242307
48.6	.024747	.476958	.000864	-	.046933	.201479	.249019
52.8	.027000	.405918	.001323	-	.056686	.258171	.250900
58.0	.028047	.313336	.002106	-	.067833	.340591	.248086
63.4	.026233	.211552	.003259	-	.076491	.446122	.236343
67.6	.021846	.130886	.004460	-	.078172	.548017	.216618
72.4	.012252	.045008	.006162	.000001	.066266	.700460	.169851
75.9	.002393	.003656	.007167	.000001	.031473	.868938	.086371

TABLE 9. Theoretical Detonation Properties of Aluminum Powder-Oxygen Mixtures (Case B)

p_1 = 1 atm

T_1 = 298.16°K

Powder oxide content = 2%

% Fuel	$\rho_1 x10^3$ (gm/cc)	u_1 (m/sec)	p_2 (atm)	T_2 (°K)	$\rho_2 x10^3$ (gm/cc)
37.5	2.09149	1744.8	30.2043	4613.3	3.90764
40.7	2.20412	1752.6	32.1060	4826.6	4.12419
43.6	2.31692	1751.9	33.8055	4991.4	4.35077
48.6	2.54304	1732.3	36.3486	5166.9	4.79222
52.8	2.76986	1703.7	37.9426	5218.0	5.18285
58.0	3.11139	1658.2	40.7535	5180.9	5.87948
63.4	3.56924	1589.9	42.5520	4906.3	6.69203
67.6	4.02992	1494.0	42.2320	4338.7	7.52509
72.4	4.72632	1346.3	40.4976	3599.5	8.86987
75.9	5.42925	1221.0	38.0528	3042.1	10.12665

TABLE 9 (Contd.)

% Fuel	Mole Fractions After Combustion							
	O(g)	O_2(g)	Al(g)	Al_2(g)	AlO(g)	Al_2O(g)	Al_2O_2(g)	Al_2O_3(g)
37.5	.389426	.267544	.003792	-	.008594	.000224	.000012	.330408
40.7	.421327	.183827	.012345	-	.017985	.000854	.000029	.363634
43.6	.421352	.126643	.030431	.000003	.030801	.002400	.000056	.388314
48.6	.363205	.066341	.089049	.000022	.055217	.008577	.000124	.417466
52.8	.281152	.036894	.159400	.000071	.071165	.018189	.000190	.432940
58.0	.161363	.014214	.264489	.000217	.079138	.039527	.000276	.440776
63.4	.042909	.002051	.377027	.000570	.060431	.092702	.000343	.423967
67.6	.003103	.000056	.397562	.001070	.023058	.220273	.000290	.354590
72.4	.000038	-	.278882	.001299	.003334	.503674	.000135	.212637
75.9	-	-	.148349	.000953	.000340	.761418	.000040	.088900

TABLE 10. Theoretical Detonation Properties of Aluminum Powder-Oxygen Mixtures (Case C)

p_1 = 1 atm
T_1 = 298.16°K
Powder oxide content = 2%

% Fuel	$\rho_1 \times 10^3$ gm/cc	u_1 m/sec	p_2 atm	T_2 °K	$\rho_2 \times 10^3$ gm/cc
30.0	1.86675	1790.9	28.8294	4674.2	3.52845
33.9	1.97903	1779.5	30.0352	4793.9	3.73027
37.5	2.09149	1763.6	30.9366	4871.8	3.91865
40.7	2.20412	1746.3	32.1860	4930.8	4.15944
43.6	2.31692	1728.9	33.1879	4972.3	4.37923
46.2	2.42989	1711.5	34.0175	5001.9	4.58461
62.2	3.45451	1585.7	41.6466	5060.9	6.56947
63.4	3.56924	1574.5	42.0066	5045.5	6.72934
65.6	3.79922	1553.3	43.9311	5015.1	7.23069
67.6	4.02922	1533.0	45.0139	4962.9	7.61670
69.3	4.26133	1513.1	46.2880	4893.0	8.04519
70.9	4.49346	1492.5	47.9448	4799.4	8.56290
72.4	4.72632	1469.6	48.8599	4660.5	9.00438
73.7	4.95990	1440.7	49.1725	4456.3	9.43185
74.9	5.19421	1400.1	47.6384	4150.0	9.69272
75.9	5.42925	1341.5	45.6868	3746.1	10.11832

TABLE 10 (Contd.)

% Fuel	Mole Fractions After Combustion							
	O(g)	O_2(g)	Al(g)	Al_2(g)	AlO(g)	Al_2O(g)	Al_2O_2(g)	Al_2O_3(liq)
30.0	.436298	.329748	.013335	.000001	.033365	.002960	.000170	.184123
33.9	.449204	.265428	.027449	.000003	.054063	.007300	.000331	.196223
37.5	.444103	.219593	.044436	.000007	.073537	.013381	.000511	.204392
40.7	.429626	.184886	.062951	.000015	.090952	.020840	.000696	.210034
43.6	.410189	.157262	.082144	.000025	.105954	.029312	.000875	.214238
46.2	.388078	.134566	.101561	.000039	.118650	.038566	.001044	.217496
-	-	-	-	-	-	-	-	-
62.2	.179699	.030920	.266351	.000319	.154843	.139804	.001888	.226176
63.4	.159394	.025456	.282272	.000364	.152200	.152853	.001913	.225547
65.6	.121500	.016612	.311985	.000475	.143812	.180375	.001928	.223314
67.6	.087677	.010054	.339325	.000598	.130848	.209643	.001871	.219984
69.3	.058380	.005445	.363407	.000742	.113586	.24[illegible]342	.001743	.215156
70.9	.034380	.002483	.383043	.000917	.092234	.277224	.001535	.208184
72.4	.016460	.000842	.396547	.001119	.067082	.318333	.001233	.198385
73.7	.005468	.000169	.399701	.001367	.040324	.368129	.000845	.183997
74.9	.000935	.000013	.385984	.001675	.017136	.431104	.000432	.162720
75.9	.000058	-	.349165	.002132	.004288	.511297	.000141	.132919

TABLE 11. Theoretical Detonation Properties of Hydrogen-Oxygen Mixtures

p_1 = 1 atm
T_1 = 298.16°K

% Fuel	$\rho_1 \times 10^4$ gm/cc	u_1 m/sec	p_2 atm	T_2 °K	$\rho_2 \times 10^3$ gm/cc
35.06	8.7806	1972.0	16.3514	3090.2	1.61271
40.12	8.1612	2085.1	16.9064	3239.1	1.49533
45.05	7.5565	2199.7	17.5781	3365.6	1.39780
50.00	6.9506	2322.7	18.0323	3472.3	1.28774
54.95	6.3434	2456.9	18.2510	3559.6	1.16715
60.00	5.7252	2609.0	18.6001	3631.9	1.05553
66.67	4.9083	2839.6	18.8805	3681.4	0.90522
69.97	4.5036	2967.5	18.8990	3675.9	0.82987
75.00	3.8872	3179.6	18.6758	3607.3	0.71422
80.00	3.2745	3406.3	18.1355	3439.5	0.60304

	Mole Fractions After Combustion					
% Fuel	O	O_2	H	H_2	OH	H_2O
35.06	.027173	.523776	.004369	.007465	.077281	.359909
40.12	.038470	.433158	.008992	.014179	.103071	.402131
45.05	.048238	.345505	.015906	.024242	.126314	.439794
50.00	.054926	.261376	.025704	.039155	.144961	.473878
54.95	.057003	.184083	.038802	.060987	.156325	.502801
60.00	.053245	.115780	.055765	.094077	.157529	.523604
66.67	.038421	.048665	.080916	.163699	.136749	.531550
69.97	.028241	.026997	.091352	.213676	.116174	.523560
75.00	.013179	.007999	.096823	.316041	.075320	.490638
80.00	.003604	.001341	.080704	.452100	.034888	.427363

TABLE 12. Measured Detonation Parameters Of Hydrogen-Oxygen Mixtures

Initial Conditions: Room Temperature
Atmospheric Pressure
Exploding Silver Wire Ignited

% Fuel	Tube Dia. (mm)	u_1 (m/sec)	p_2 (atm)
40.0	26.4	2072	16.9
40.0	26.4	-	17.6
42.8	26.4	2158	17.0
45.0	26.4	2264	16.6
45.0	26.4	2264	16.1
45.1	26.4	-	16.5
50.0	26.4	2363	15.4
50.0	26.4	-	16.4
52.4	26.4	2376	17.0
54.9	26.4	-	16.3
58.8	26.4	2533	17.0
58.8	26.4	2564	17.9
60.0	26.4	-	16.4
60.1	26.4	-	17.1
60.1	26.4	-	16.3
60.2	26.4	2637	-
63.2	26.4	2687	17.0
66.8	26.4	2894	17.4
70.0	26.4	-	15.5
70.0	26.4	-	15.9
75.0	26.4	-	16.8
79.0	26.4	-	19.5

TABLE 13. Measured Flame Temperatures* of Granular Aluminum Powder-Oxygen Mixtures

Initial Conditions: Room Temperature Atmospheric Pressure

% Fuel	Temp. (°K)	% Fuel	Temp. (°K)
49.3	3560	58.8	3715
49.3	3605	62.9	3795
51.0	3660	66.2	3560
54.1	3780	70.0	3660

*From FeI Lines

TABLE 14. Measured Burning Velocities** Of Aluminum Powder-Oxygen Mixtures

Initial Conditions: Room Temperature Atmospheric Pressure

% Fuel	Powder	Su (cm/sec)	% Fuel	Powder	Su (cm/sec)
41.7	flake	30.3	46.5	flake	21.0
43.1	flake	30.0	46.5	flake	19.5
43.3	flake	27.0	49.3	flake	19.8
43.3	flake	23.0	61.3	granular	26.4
45.7	flake	30.1	62.9	granular	24.2
45.7	flake	21.0	64.5	granular	17.2
46.5	flake	29.2	64.5	granular	24.5
46.5	flake	27.0	64.5	granular	29.0
46.5	flake	24.5	71.4	granular	20.5

**Bunsen-burner Method